Supplementary information

DNA-Assisted Assembly of Cationic Gold Nanoparticles: Monte Carlo Simulation

Ambroise de Izarra,[a,b] Yun Hee Jang,[a] and Yves Lansac[b,c]

[a] Department of Energy Science and Engineering, DGIST, Daegu 42988, Korea
[b] GREMAN, UMR 7347, CNRS, Université de Tours, 37200 Tours, France
[c] Laboratoire de Physique des Solides, CNRS, Université Paris-Saclay, 91405 Orsay, France

‡ E-mail: ambroise.deizarra@univ-tours.fr, lansac@univ-tours.fr, yhjang@dgist.ac.kr

S1 Construction of the Coarse-grained AuNP

In order to study the influence of the AuNP charge distribution, we consider different variants of our model with different number and disposition of the ligands on the gold core such that AuNP will carry either 6, 12 or 30 ligands for a charge density of 0.97, 1.94 and 4.87 |e| nm^{-2} respectively.

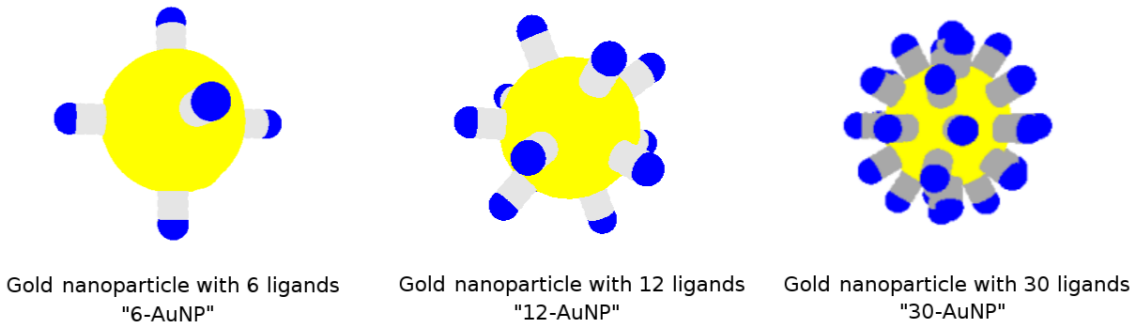

Figure S1: CG model of AuNP with 6, 12 or 30 ligands.

The Figure S1 presents the three different types of AuNPs with their ligands disposed on the gold core. The way to homogeneously distribute the ligands on the CG gold surface for the different models of AuNP is done in the following way.

- For the AuNP model with 6 ligands (i.e, 6-AuNP), positions are chosen according to the following Euler angles:

$$\theta = 0 \quad , \qquad \phi = 0 \tag{1}$$
$$\theta = \frac{\pi}{2} \quad , \qquad \phi = \tfrac{\pi}{4} \times i \quad i = (0,1,2,3) \tag{2}$$
$$\theta = \pi \quad , \qquad \phi = 0 \tag{3}$$

- For the 12-AuNP model, the ligands are placed on the gold core according to:

$$\theta = \frac{\pi}{6} \quad , \qquad \phi = \tfrac{2\pi}{3} \times i \quad i = (0,1,2) \tag{4}$$
$$\theta = \frac{\pi}{2} \quad , \qquad \phi = \tfrac{\pi}{6} \times i \quad i = (0,1,2,3,4,5) \tag{5}$$
$$\theta = \frac{5\pi}{6} \quad , \qquad \phi = \tfrac{\pi}{6} + \tfrac{2\pi}{3} \times i \quad i = (0,1,2) \tag{6}$$

- Finally, the rules to distribute the ligands on the 30-AuNP model write as:

$$\theta = 0 \quad , \qquad \phi = 0 \tag{7}$$
$$\theta = \frac{\pi}{6} \quad , \qquad \phi = \tfrac{2\pi}{3} \times i \quad i = (0,1,2) \tag{8}$$
$$\theta = \frac{\pi}{3} \quad , \qquad \phi = \tfrac{\pi}{6} \times i \quad i = (0,1,2,3,4,5) \tag{9}$$
$$\theta = \frac{\pi}{2} \quad , \qquad \phi = \tfrac{\pi}{5} \times i \quad i = (0,1,2,3,4,5,6,7,8,9) \tag{10}$$
$$\theta = \frac{2\pi}{3} \quad , \qquad \phi = \tfrac{\pi}{6} + \tfrac{\pi}{6} \times i \quad i = (0,1,2,3,4,5) \tag{11}$$
$$\theta = \frac{5\pi}{6} \quad , \qquad \phi = \tfrac{\pi}{6} + \tfrac{2\pi}{3} \times i \quad i = (0,1,2) \tag{12}$$
$$\theta = \pi \quad , \qquad \phi = 0 \tag{13}$$

S2 The Ewald summation technique

S2.1 Expression of the electrostatic interactions

The Ewald summation method is used to compute the electrostatic energy in a periodic system. The idea of the Ewald summation algorithm is to split the low converging electrostatic potential into two converging sub-potentials.[1]

The original set composed of point charges is modified by introducing gaussian charges ("clouds") of opposite charge such that the lattice becomes neutral as shown in Figure S2, lattice B. In order

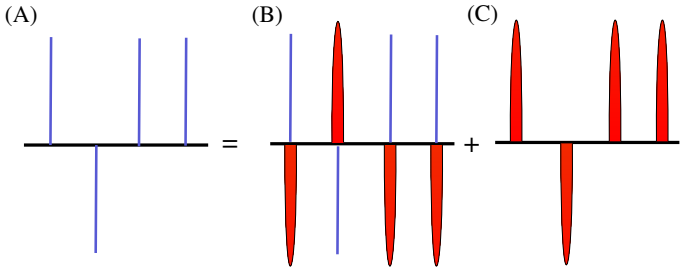

Figure S2: (A) The original set of electrostatic charges (in blue) is separated into two sets of charges. (B) Each charge is associated with a diffuse opposite charge (in red). (C) The diffuse opposite charges are withdrawn so that (A) = (B)+(C) in term of electrostatic charge.

to evaluate only the contribution of the point charges (lattice A), it is required to add a lattice of compensate diffuse charges of the same sign as the point charges (Figure S2, lattice C). The electrostatic energy produced by lattice B will decay thus faster and can be computed using a cutoff scheme. This contribution to the electrostatic energy is computed in the **r**-space, while the contribution of the lattice C is calculated in the **k**-space.

The total electrostatic energy can thus be written as the sum of three terms:

$$\mathcal{U}^{EL} = \mathcal{U}^{SR} + \mathcal{U}^{LR} + \mathcal{U}^{Self} \tag{14}$$

The long range interaction energy $\mathcal{U}^{LR}$ is expressed as follows:

$$\mathcal{U}^{LR} = \frac{1}{2\pi V} \sum_{\mathbf{k}\neq\mathbf{0}} \frac{1}{4\pi\epsilon_o k^2} \exp\left[-\left(\frac{\pi k}{\alpha}\right)^2\right] \cdot \left|\sum_{i=1}^{N} q_i \exp\left(2\pi i \mathbf{k}\cdot\mathbf{r}_i\right)\right|^2 \tag{15}$$

The short range contribution $\mathcal{U}^{SR}$ is calculated up to a cut-off in the real space:

$$\mathcal{U}^{SR} = \frac{1}{2}\sum_{i\neq j}^{N} \frac{q_i q_j}{4\pi\epsilon_o} \frac{erfc(\alpha r_{ij})}{r_{ij}} \Theta(r_{cut} - r_{ij}) \tag{16}$$

There is a supplemental term $\mathcal{U}^{Self}$ taking into account the interaction of the gaussian distribution with itself:

$$\mathcal{U}^{Self} = -\frac{\alpha}{\sqrt{\pi}} \sum_{i=1}^{N} q_i^2 \tag{17}$$

In order to use the Ewald method, three parameters need to be chosen:

- the real cutoff parameter r_{cut},
- the cutoff lattice vector in the reciprocal space n_c,
- the splitting parameter α.

The short-range energy must vanish at the cutoff r_{cut}.[2] In that case, the short-range potential varies like:

$$\mathcal{U}^{SR} \propto \frac{\exp\left(-\alpha^2 r_c^2\right)}{(\alpha r_c)^2} \tag{18}$$

The long range energy also depends of a decaying exponentiel term:

$$\mathcal{U}^{LR} \propto \frac{\exp\left[-\left(\frac{\pi n_c}{\alpha L}\right)^2\right]}{\left(\left(\frac{\pi n_c}{\alpha L}\right)^2\right.} \tag{19}$$

Each contribution varies like $\frac{\exp(-x^2)}{x^2}$. Let us denote s the value such that $\frac{\exp(-s^2)}{s^2} = \epsilon$. By identifying this with equations 18 and 19, we obtain the two following relations:

$$\begin{cases} \alpha = \frac{s}{r_{cut}} \\ n_c = \frac{sL\alpha}{\pi} \end{cases} \tag{20}$$

In our simulations, we have chosen $s = 3$ which corresponds to $\epsilon \approx 10^{-5}$ and $r_{cut} = \frac{min(L_x, L_y, L_z)}{2}$. For this choice of parameters of s and r_{cut}, the damping parameter α and n_c become for a cubic box of side L:

$$\begin{cases} \alpha = \frac{6}{L} \\ n_c = \frac{18}{\pi} \approx 6 \end{cases} \tag{21}$$

S2.2 Expression of the electrostatic Forces

In addition to the implementation of the Ewald summation technique in our MC simulation package, it is necessary to derive the electrostatic forces from the Ewald energy to perform further analysis. The electrostatic force acting on particle i from all other particles j in the system[2] (and all their images in the image cells taking into account PBCs) is expressed as:

$$\mathbf{F}_i^{EL} = -\vec{\nabla}_{\mathbf{r}_i}\mathcal{U}^{EL} = \mathbf{F}^{SR} + \mathbf{F}^{LR} = -\vec{\nabla}_{\mathbf{r}_i}\mathcal{U}^{SR} - \vec{\nabla}_{\mathbf{r}_i}\mathcal{U}^{LR} \tag{22}$$

We notice that $\mathcal{U}^{Self}$ does not depend on coordinates and vanish. The differentiation of the short-range electrostatic energy leads to the short-range electrostatic forces:

$$\mathbf{F}^{SR} = -\vec{\nabla}_{\mathbf{r}_i}\mathcal{U}^{SR} \tag{23}$$

$$\mathbf{F}^{SR} = -\vec{\nabla}_{\mathbf{r}_i}\left[\frac{1}{2}\sum_{i\neq j}^{N}\frac{q_i q_j}{4\pi\epsilon_o}\frac{erfc(\alpha r_{ij})}{r_{ij}}\right] \tag{24}$$

$$\mathbf{F}^{SR} = -\left[\frac{1}{2}\sum_{i\neq j}^{N}\frac{q_i q_j}{4\pi\epsilon_o}\left[\vec{\nabla}_{\mathbf{r}_i}\left(\frac{1}{r_{ij}}\right)erfc(\alpha r_{ij}) + \frac{1}{r_{ij}}\vec{\nabla}_{\mathbf{r}_i}\left(erfc(\alpha r_{ij})\right)\right]\right] \tag{25}$$

$$\mathbf{F}^{SR} = -\left[\frac{1}{2}\sum_{i\neq j}^{N}\frac{q_i q_j}{4\pi\epsilon_o}\left[-\left(\frac{\mathbf{r}_{ij}}{r_{ij}^3}\right)erfc(\alpha r_{ij}) + \frac{1}{r_{ij}}\left(-\frac{2\alpha}{\sqrt{\pi}}\exp\left(-(\alpha r_{ij}^2)\right)\frac{\mathbf{r}_{ij}}{r_{ij}}\right)\right]\right] \tag{26}$$

$$\mathbf{F}^{SR} = q_i\sum_{i>j}^{N}q_j\left[\frac{2\alpha}{\sqrt{\pi}}\exp\left(-(\alpha r_{ij})^2\right) + \frac{erfc(\alpha r_{ij})}{r_{ij}}\right]\frac{\mathbf{r}_{ij}}{r_{ij}^2} \tag{27}$$

In the same manner, let us derive the long-range part of the electrostatic Forces.
In order to be clearer, let us call:

$$\sum_{i=1}^{N}q_i\exp\left(2\pi i\mathbf{k}\cdot\mathbf{r}_i\right) = \rho(\mathbf{k}) \tag{28}$$

If we apply the gradient operator to $\rho(\mathbf{k})$, we obtain the useful relation:

$$\vec{\nabla}_{\mathbf{r}_i}\rho(\mathbf{k}) = \delta_{ij}q_j 2\pi i\mathbf{k}\exp\left(2\pi i\mathbf{k}\cdot\mathbf{r}_j\right) \tag{29}$$

Finally the long-range electrostatic forces $\mathbf{F}^{LR}$ writes:

$$\mathbf{F}^{LR} = \ -\vec{\nabla}_{\mathbf{r}_i}\mathcal{U}^{LR} \tag{30}$$

$$\mathbf{F}^{LR} = -\vec{\nabla}_{\mathbf{r}_i}\left[\frac{1}{2\pi V}\sum_{\mathbf{k}\neq\mathbf{0}}\frac{1}{4\pi\epsilon_o k^2}\exp\left[-\left(\frac{\pi k}{\alpha}\right)^2\right]\cdot|\rho(\mathbf{k})|^2\right] \tag{31}$$

$$\mathbf{F}^{LR} = -\left[\frac{1}{2\pi V}\sum_{\mathbf{k}\neq\mathbf{0}}\frac{1}{4\pi\epsilon_o k^2}\exp\left[-\left(\frac{\pi k}{\alpha}\right)^2\right]\right]\cdot\vec{\nabla}_{\mathbf{r}_i}\left|\rho(\mathbf{k})\right|^2 \tag{32}$$

$$\mathbf{F}^{LR} = -\left[\frac{1}{2\pi V}\sum_{\mathbf{k}\neq\mathbf{0}}\frac{1}{4\pi\epsilon_o k^2}\exp\left[-\left(\frac{\pi k}{\alpha}\right)^2\right]\right]\cdot\left[2\pi i q_i\mathbf{k}\left[\sum_{j=1}^{N}2\pi i q_j\sin\left(\mathbf{k}\cdot\mathbf{r}_{ij}\right)\right]\right] \tag{33}$$

$$\mathbf{F}^{LR} = \frac{q_i}{4\pi\epsilon_o}\sum_{j=1}^{N}\left[\frac{2q_j}{V}\sum_{\mathbf{k}\neq\mathbf{0}}\left[\frac{\exp\left(-\left(\frac{\pi k}{\alpha}\right)^2\right)}{k^2}\sin\left(2\pi\mathbf{k}\cdot\mathbf{r}_{ij}\right)\mathbf{k}\right]\right] \tag{34}$$

The Ewald summation method is only suitable to compute the electrostatic interactions for relatively small systems of at most several hundreds charges, which is the case in this work.

S3 The Monte Carlo simulation package

We provide a brief presentation of the Monte Carlo simulation package we have developed. Although the main core is the Monte Carlo program, we implemented additional programs to construct the initial configurations of the systems, to associate the radius and charges for beads (i.e, the force field) and to visualize and analyze the output trajectory. The description of the workflow between the different programs is presented in Figure S3.

We first construct the system using the "Initialization_system.cpp" program which creates a file "System_construct.txt" with the name of each moities (ions, bead and molecules), their coordinates and the connectivity between each bead.

The "Building_topology.cpp" program reads inputs from the "System_construct.txt" file and reads force field parameters (bead radius and charges) from "Radius_particles.txt" and "Electrostatic_charges.txt". The created output files contain the list of the beads and their initial coordinates in "System_geometry.txt" and a list of each bead with their corresponding charge and radius in "System_topology.txt".

The core of the simulation package performing a Monte Carlo simulation is implemented in "Main_MC.cpp", the master program used to initialize the classes and parameters for the three other .cpp files. The "Move_MC.cpp" is the program where the different Monte Carlo moves and the associated acceptance probabilities are implemented. The "Potential_energy_calculation.cpp" file computes the change of energy after a proposed MC move. Finally, "the Cell_lists.cpp" program manages the cell lists through the whole simulation.

Once we get the trajectory of the system during the MC simulation ("Traj_output.txt"), we can either visualize it with "Visualization_trajectory.cpp" or analyse it with "Analysis_trajectory.cpp". The trajectory file can be read with "Read_trajectory.cpp".

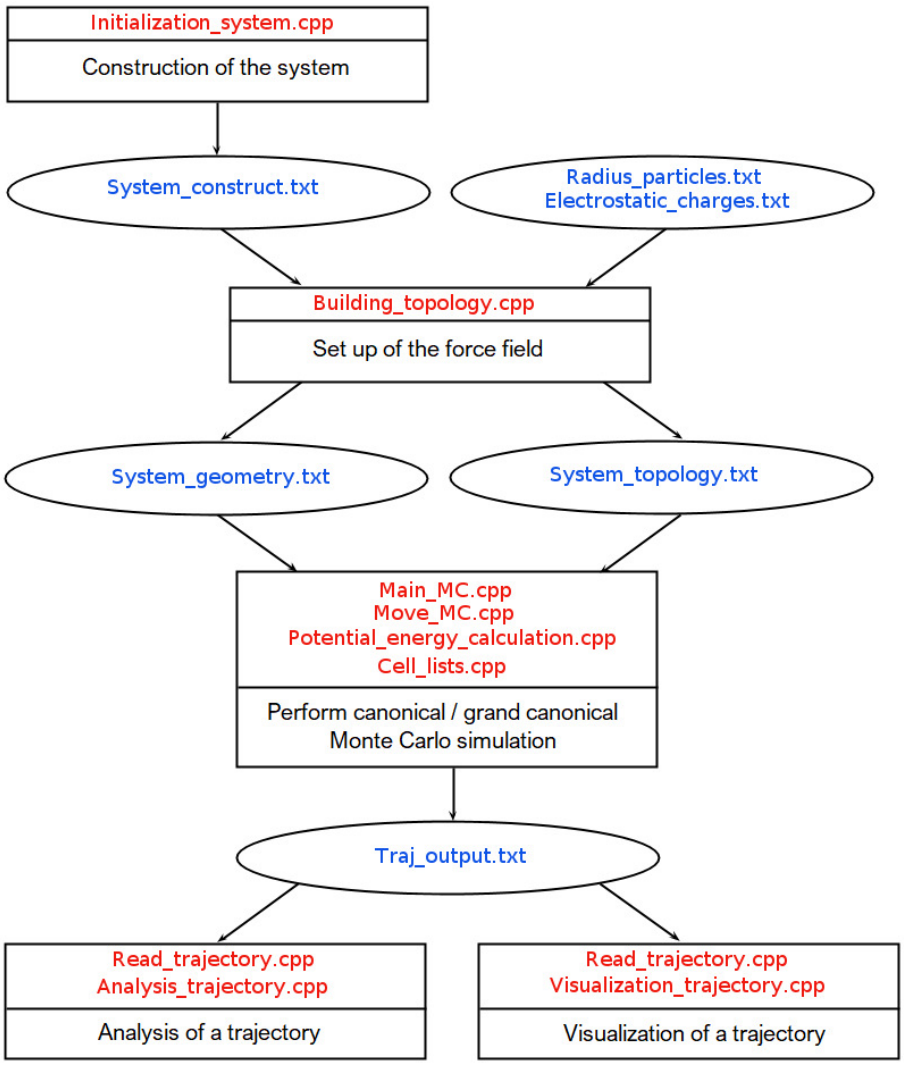

Figure S3: Description of the package we developed and implemented to perform a complete Monte Carlo simulation, from the construction of the system to the analysis of an output trajectory.

S4 Adsorption of AuNPs on a DNA: supplementary calculations

S4.1 Adsorbed species on a DNA for systems containing 12-AuNPs and 30-AuNPs

We determine the adsorbed species on a single DNA and coordination number of the different species in the simulation box for the systems containing the 12-AuNPs and the 30-AuNPs (see Table 1, Section 3.1 of main text for composition of the systems), presented respectively in Figure S4 and Figure S5.

At $R_{+/-} = 0.5$-1.0, all the 12-AuNPs or the 30-AuNPs are adsorbed on the DNA (Figures S4a

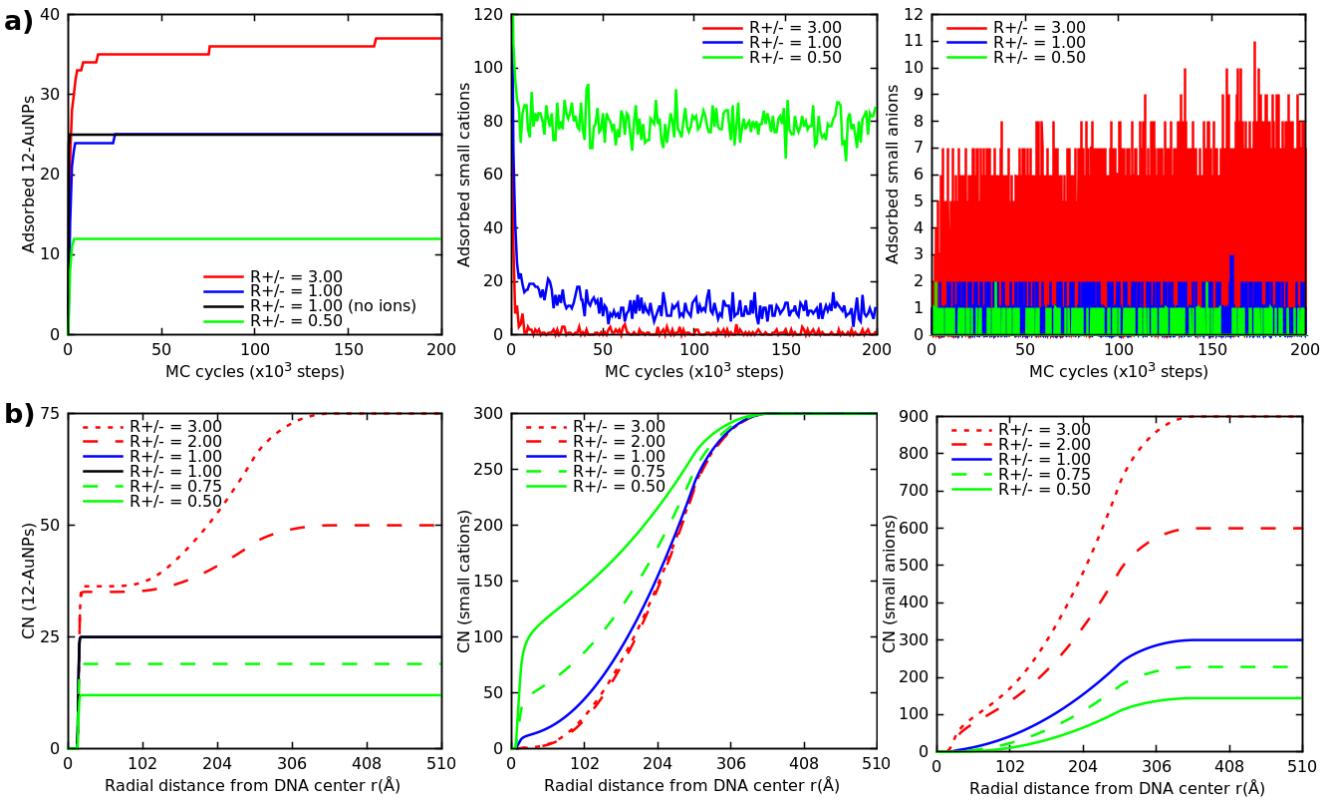

Figure S4: a) Number of adsorbed species on the DNA during the MC simulations at different $R_{+/-}$ (left: number of 12-AuNPs, middle: number of counter-cations, right: number of counter-anions). b) Coordination number (CN) as a function of distance from the DNA axis at various $R_{+/-}$ (left: CN of 12-AuNPs, middle: CN of counter-cations, right: CN of counter-anions).

and S5a, left plots, green, black and blue curves). Because of the higher electrostatic repulsion between the 12-AuNPs or 30-AuNPs than between the 6-AuNPs, the DNA are not fully covered by the AuNPs and there are respectively 36 12-AuNPs and 20 30-AuNPs adsorbed on the DNA at $R_{+/-} = 3.0$. Again, we found that when AuNPs adsorb on the DNA, the counter-cations are depleted from its surface as shown by middle curves of Figures S4a and S5a and a small fraction of counter-anions stick to AuNPs adsorbed on the DNA (Figures S4a and S5a, right curves).

The coordination number of the different species in systems containing 12-AuNPs and 30-AuNPs follow the trend of the systems containg the 6-AuNPs (Figures S4b and S5b, left curves). The CN for the AuNPs is constant up to 100 Å because of the electrostatic repulsion exerted between the adsorbed AuNPs on DNA and the surrounding AuNPs in the bulk. A higher fraction of AuNPs adsorbed on the DNA is consistent with a fall of the CN of counter-cations at short distance (Figures S4b and S5b, middle curves). The region where the CN of AuNPs is constant (up to r $\sim$ 100 Å) is rather populated by counter-anions as shown by the increase of the corresponding CN (Figures S4b and S5b, right curves).

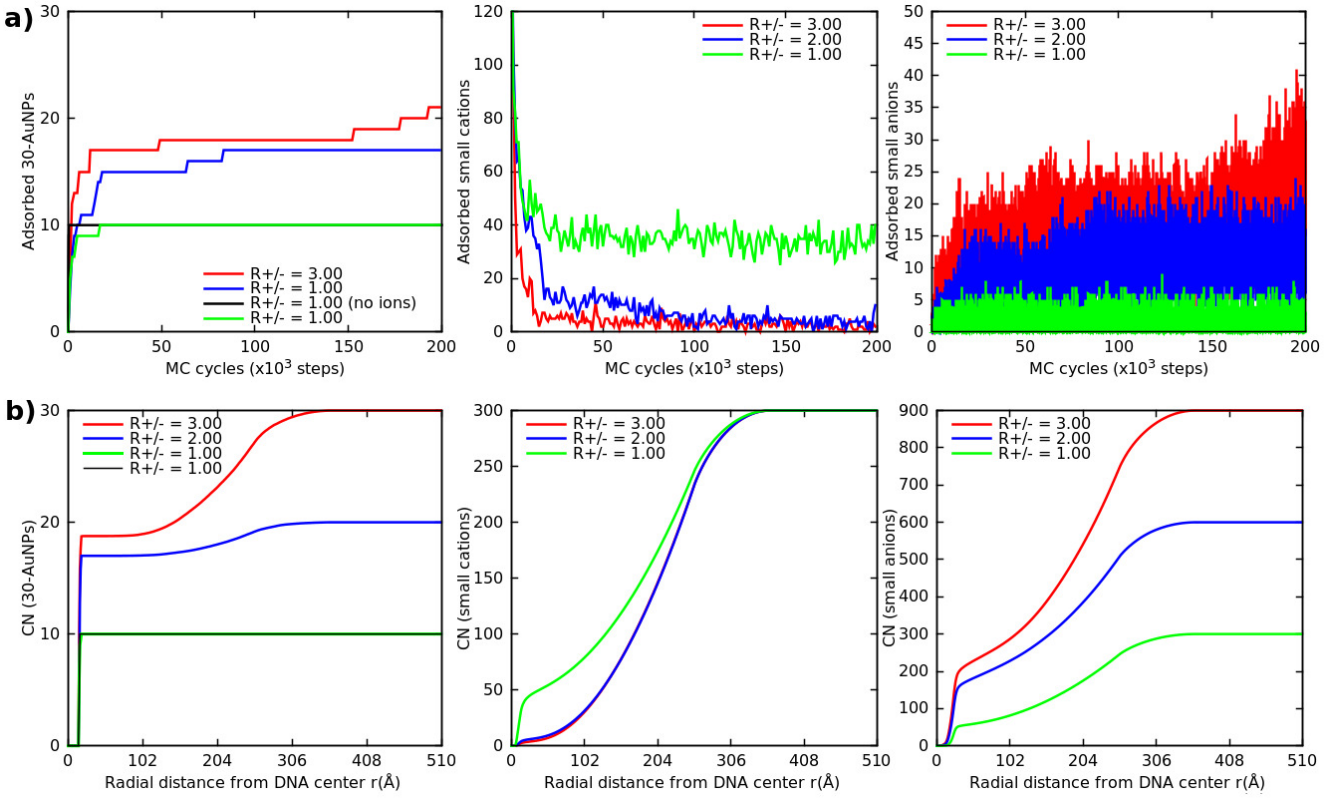

Figure S5: a) Number of adsorbed species on the DNA during the MC simulations at different $R_{+/-}$ (left: number of 30-AuNPs, middle: number of counter-cations, right: number of counter-anions). b) Coordination number (CN) as a function of distance from the DNA axis at various $R_{+/-}$ (left: CN of 30-AuNPs, middle: CN of counter-cations, right: CN of counter-anions).

S4.2 Overcharging effect

By using the CN curves of each species, we calculated the charge compensation to probe the influence of the adsorbed AuNPs, counter-cations and counter-anions on the DNA effective charge experienced at a given radial distance. The charge compensation is defined as the radial integrated charge from the DNA axis[3] shown in Figure S6. The term q_{AuNP} denotes the number of charge carried by the AuNPs:

$$\theta(r) = |e| \left[-CN_{phos}(r) + CN_{cation}(r) - CN_{anion}(r) + q_{AuNP} \times CN_{AuNP}(r) \right] \tag{35}$$

The charge compensation is positive at short distance (< 8.5 Å) due to counter-cations populating grooves and strands of the DNA. After this maximum, a drop is observed due to the integrated density of DNA negative phosphate groups located at a radial distance $r = 8.9$ Å from the DNA axis. When r is progressively increased, the effective charge increases and for excess of AuNPs ($R_{+/-} = 2.0$-3.0) not only the AuNPs compensate the DNA charge, but exceed it resulting in opposite values of integrated charge (i.e., charge inversion) at some distance and apparition of

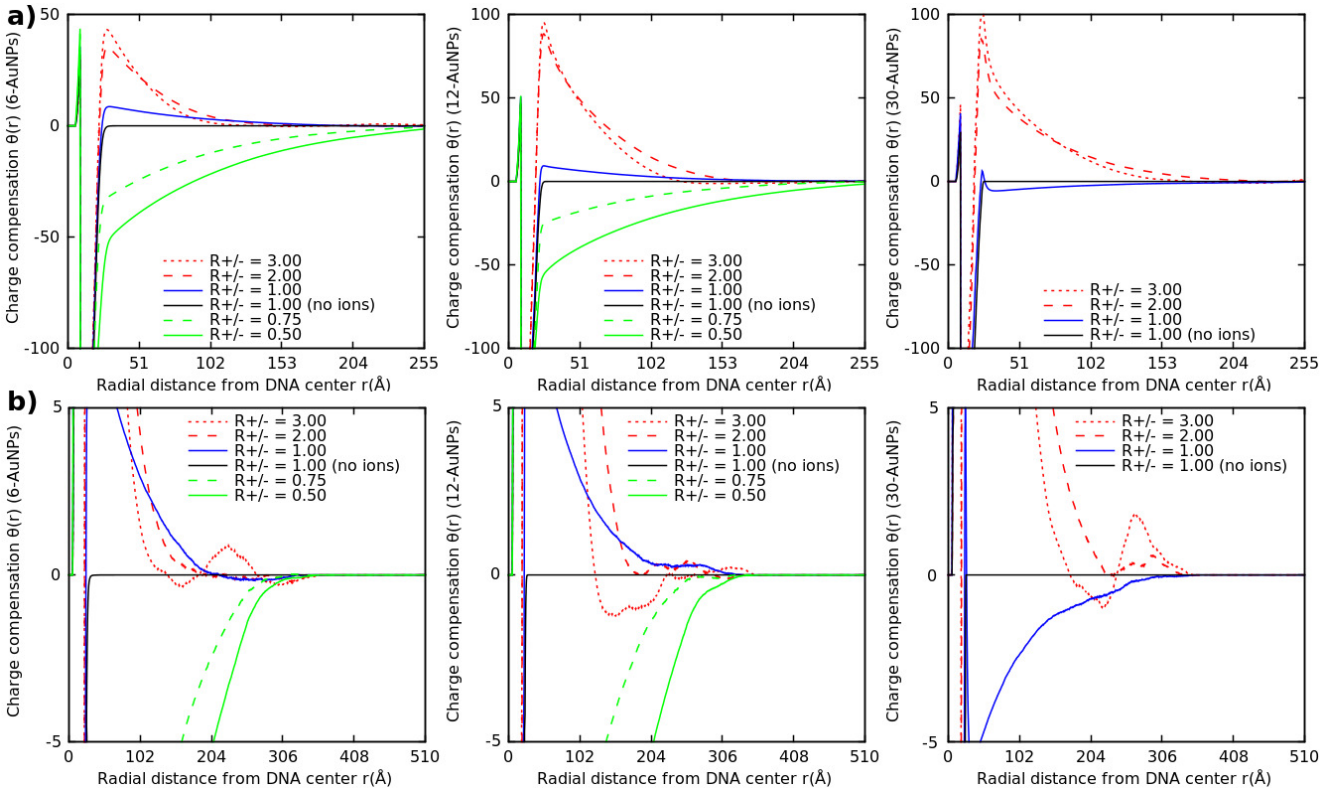

Figure S6: a) Charge compensation θ(r) versus radial distance from DNA axis for systems with different model of AuNPs at different $R_{+/-}$. b) Zoom of the charge compensation θ(r).

layers of opposite charges. We remark that the onset of overcharging effect begins even at $R_{+/-} = 1.0$, with significant amount of counter-cations adsorbed on DNA in addition to the totality of the 6-AuNPs and 12-AuNPs compensating exactly the DNA charge (blue curves in left and middle plots, Figure S6a,b). For systems containing the 30-AuNPs, there is a drop of the charge compensation near the DNA surface at $R_{+/-} = 1.0$ (blue curves in right plots, Figure S6a,b), because anions tend to stick to the 30-AuNPs surface. It has been shown that rodlike polyelectrolytes like DNA can undergo a charge reversal in presence of an excess of condensed multivalent counterions both experimentally[4] or thanks to numerical simulations.[3,5] In our systems, the overcharging effect arises with the condensation of AuNPs while a second layer associated to the reversal charge around $r \sim$150 Å is due to the attracted anions screening the first layer of charge carried by the AuNPs adsorbed on the DNA.[6]

S4.3 Helical projections of species in 12-AuNPs and 30-AuNPs systems

The helical projections for species in systems containing the 12-AuNPs and 30-AuNPs are presented in Figure S7.

Like for the helical projection of the 6-AuNPs, the distribution of 12-AuNPs and 30-AuNPs

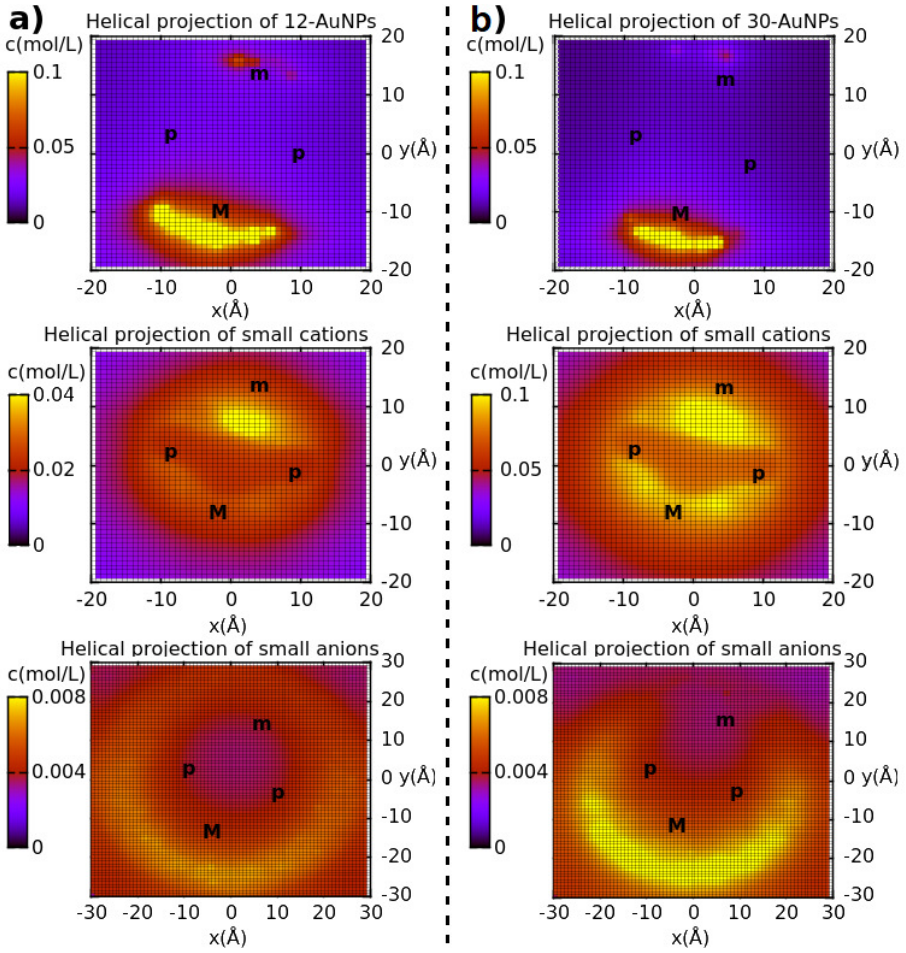

Figure S7: Helical projection of densities (mol L^{-1}) of each species, (top) AuNPs, (middle) counter-cations, and (bottom) counter-anions, adsorbed on DNA at $R_{+/-} = 1.0$. The indices "**m**", "**M**", and "**S**" indicate minor groove, major groove, and phosphate, respectively. a) Systems containing 12-AuNPs. b) Systems containing 30-AuNPs.

is the highest in the major groove (top plots in Figure S7a,b) while the counter-cation density is higher in the minor groove in all cases (middle plots in Figure S7a,b) revealing clearly the shape of DNA.[7] The counter-anion distribution around the DNA molecule is shown at the bottom of Figure S7a,b. The anion density remains low in the DNA vicinity but When the charge of the AuNP is increased, an outer layer made of small counter-anions emerges in the major groove, corresponding to anions adsorbed at the AuNPs surface.

S4.4 Distribution of 12-AuNPs adsorbed on the DNA

The distance along DNA long-axis between closest adsorbed 12-AuNPs is estimated by calculating the corresponding normalized histogram of the consecutive 12-AuNP distance (Figure S8).

At the isoelectric point ($R_{+/-} = 1.0$), the histograms display a maximum at ~ 20 Å , consistent

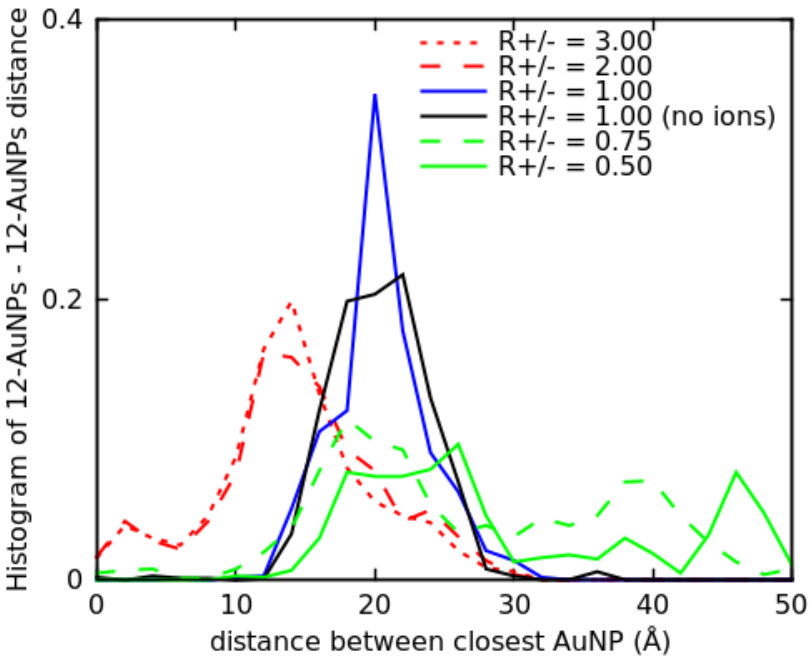

Figure S8: Histogram of the nearest-neighbor distance along the DNA long axis between 12-AuNPs bound to DNA.

with a spacing distance of $\frac{510}{25} = 20.4$ Å if the 12-AuNPs are evenly spaced along the DNA. For $R_{+/-} = 0.5$-0.75, the distribution is broader. Indeed, in addition to a fewer number of 12-AuNPs adsorbed on DNA compared to the simulations involving the 6-AuNPs, a layer of counter-anions adsorb at the surface of the 12-AuNPs due to their higher charge density and screen the AuNP-AuNP repulsion. Such effect can disturb the distribution of the 12-AuNPs along the DNA. The systems with an excess of 12-AuNPs behave in a way similar than those with an excess of 6-AuNPs. At $R_{+/-} = 2.0$-3.0, the most probable consecutive distance is 14 Å which is equivalent to the distance of $\frac{510}{37} \approx 13.8$ Å if the ~ 37 adsorbed 12-AuNPs are evenly spaced along the DNA (left plots in Figure S4a).

S5 Estimation of error of effective force between two DNA-AuNP complexes

We provide an estimation of the error associated to the calculation of the effective forces between the pair of DNA decorated by AuNPs presented in the section 3.2 of the main text. The Monte Carlo simulation method yields to approximate results and the accuracy depends on the number of values N used to calculate the average of a given quantity A. The determination of the error is based on the calculation of the variance σ^2 defined as:

$$\sigma^2 = \left\langle A^2 \right\rangle - \langle A \rangle^2 \tag{36}$$

where the average of the observable A writes:

$$\langle A \rangle \quad = \quad \frac{1}{N} \sum_{i=1}^{N} A_i \tag{37}$$

and the average of the square of A writes:

$$\left\langle A^2 \right\rangle \quad = \quad \frac{1}{N} \sum_{i=1}^{N} (A_i)^2 \tag{38}$$

The standard deviation is given by the square root of the variance $\sqrt{\sigma^2}$. However, it is expected that the error decreases with the number of points N which is not the case by using equation 36. Instead, from a simulation where we extracted N measures, we divide the set of measures into L blocks containing $M = N/L$ measures[2] and we compute the average for each block of size M as follows:

$$\langle A \rangle_k \quad = \quad \frac{1}{M} \sum_{i=M*(k-1)+1}^{M*k} A_i \tag{39}$$

where k varies from 1 to L. We ensure that the size of the block are higher than the correlation length calculated by the auto-correlation function c(l) defined as:

$$c(l) \quad = \quad \frac{1}{N-l} \sum_{i=1}^{N-l} (A_i - \langle A \rangle)(A_{(i+l)} - \langle A \rangle) \tag{40}$$

Finally the error Δ_A is calculated by computing the "standard deviation of the means" denoted by σ_M:

$$\Delta_A = \sqrt{\sigma_M} \quad = \quad \sqrt{\langle I^2 \rangle - \langle I \rangle^2} \tag{41}$$

where the average of the new observable I writes:

$$\langle I \rangle = \frac{1}{L} \sum_{k=1}^{L} \langle A \rangle_k \tag{42}$$

and the average of the square of I writes:

$$\left\langle I^2 \right\rangle = \frac{1}{L} \sum_{k=1}^{L} \langle A \rangle_k^2 \tag{43}$$

In the analysis, we have chosen $L = 10$. The error for the effective force and each contribution to the effective force for systems containing 6-AuNPs and 12-AuNPs are given in Tables S1-S8.

Table S1: Effective force exerted between the DNA pair in presence of 6-AuNPs at $R_{+/-} = 0.5$ corresponding to 20 AuNPs, 240 counter-cations and 120 counter-anions in the system.

ℓ(Å)	F/F$_o$	F$_1$/F$_o$	F$_2$/F$_o$	F$_3$/F$_o$	F$_4$/F$_o$
20	98.6 ± 1.6	310.7 ± 0.0	-127.4 ± 6.6	-3.1 ± 0.1	-81.6 ± 12.4
22	45.0 ± 4.0	256.6 ± 0.0	-115.2 ± 9.5	-3.5 ± 0.1	-92.9 ± 22.1
24	22.8 ± 4.9	229.6 ± 0.0	-99.3 ± 23.6	-3.3 ± 0.1	-104.2 ± 48.5
26	8.7 ± 3.9	209.5 ± 0.0	-81.2 ± 4.9	-3.7 ± 0.1	-115.9 ± 17.2
28	-7.0 ± 14.1	192.6 ± 0.0	-53.7 ± 25.6	-3.9 ± 0.1	-142.0 ± 76.5
30	-15.9 ± 12.8	178.1 ± 0.0	-37.0 ± 26.9	-3.7 ± 0.1	-153.3 ± 77.8
32	-18.7 ± 1.7	165.2 ± 0.0	-36.1 ± 8.9	-4.3 ± 0.2	-143.5 ± 8.1
34	-18.0 ± 2.8	153.8 ± 0.0	-34.4 ± 4.3	-4.3 ± 0.2	-133.1 ± 11.0
36	-14.5 ± 3.5	143.5 ± 0.0	-35.1 ± 10.5	-4.3 ± 0.2	-118.6 ± 24.9
38	-10.0 ± 6.6	134.2 ± 0.0	-38.9 ± 5.7	-4.6 ± 0.6	-100.7 ± 29.0
40	-6.9 ± 1.5	125.7 ± 0.0	-40.0 ± 3.1	-3.8 ± 0.3	-88.8 ± 9.6
42	-4.6 ± 1.6	117.9 ± 0.0	-39.6 ± 4.8	-4.1 ± 0.4	-78.8 ± 11.1
44	-3.0 ± 5.9	110.7 ± 0.0	-39.0 ± 16.0	-3.8 ± 0.4	-70.9 ± 40.7
46	-1.8 ± 1.3	104.0 ± 0.0	-40.0 ± 4.5	-3.6 ± 0.3	-62.2 ± 8.1
48	-2.9 ± 1.8	97.8 ± 0.0	-35.5 ± 7.7	-3.7 ± 0.3	-61.5 ± 14.7
50	-1.7 ± 3.2	92.0 ± 0.0	-36.4 ± 15.4	-4.3 ± 1.8	-53.0 ± 41.2
52	-1.6 ± 3.8	86.5 ± 0.0	-33.5 ± 9.0	-3.2 ± 0.2	-51.4 ± 26.2
54	-0.4 ± 4.0	81.4 ± 0.0	-32.6 ± 9.9	-3.3 ± 0.9	-45.9 ± 22.1
56	0.3 ± 1.7	76.5 ± 0.0	-32.2 ± 8.4	-3.5 ± 0.5	-40.5 ± 12.1
58	-1.4 ± 2.8	71.9 ± 0.0	-27.5 ± 6.3	-3.3 ± 0.8	-42.5 ± 19.1
60	-0.8 ± 3.7	67.5 ± 0.0	-27.6 ± 6.0	-2.8 ± 0.9	-37.9 ± 21.2
62	-0.4 ± 1.5	63.3 ± 0.0	-25.8 ± 6.0	-2.7 ± 0.6	-35.2 ± 11.9
64	-0.7 ± 3.7	59.3 ± 0.0	-23.7 ± 20.6	-2.6 ± 0.7	-33.7 ± 43.3
66	0.1 ± 2.9	55.4 ± 0.0	-24.6 ± 9.0	-2.8 ± 0.6	-27.9 ± 22.2
68	0.6 ± 1.5	51.7 ± 0.0	-21.8 ± 11.2	-3.6 ± 0.3	-25.7 ± 16.9
70	-1.1 ± 21.0	48.1 ± 0.0	-21.3 ± 5.1	-2.4 ± 1.2	-25.5 ± 29.8
72	0.7 ± 5.5	44.6 ± 0.0	-20.0 ± 14.7	-1.8 ± 1.2	-22.1 ± 40.9
74	0.7 ± 7.2	41.2 ± 0.0	-16.8 ± 19.9	-2.1 ± 0.7	-21.6 ± 27.2
76	0.5 ± 8.1	38.0 ± 0.0	-14.1 ± 37.3	-1.8 ± 1.1	-21.6 ± 32.8
78	-0.1 ± 3.4	34.8 ± 0.0	-14.7 ± 12.7	-2.0 ± 1.9	-18.2 ± 22.3
80	0.0 ± 5.5	31.6 ± 0.0	-14.1 ± 7.7	-1.4 ± 1.2	-16.1 ± 30.4
82	-1.1 ± 4.8	28.6 ± 0.0	-10.1 ± 11.3	-1.8 ± 2.3	-17.8 ± 30.8
84	-1.3 ± 3.2	25.5 ± 0.0	-9.0 ± 6.6	-0.8 ± 1.7	-17.0 ± 24.9
86	0.4 ± 2.1	22.6 ± 0.0	-10.7 ± 4.8	-1.0 ± 0.8	-10.5 ± 13.0
88	0.3 ± 5.4	19.7 ± 0.0	-10.2 ± 28.4	-1.4 ± 2.5	-7.8 ± 53.8
90	-0.5 ± 3.8	16.8 ± 0.0	-7.2 ± 6.2	-0.5 ± 0.9	-9.6 ± 23.9
92	0.4 ± 3.1	13.9 ± 0.0	-6.3 ± 12.8	-1.2 ± 1.6	-6.0 ± 22.7
94	0.8 ± 3.6	11.1 ± 0.0	-6.2 ± 12.3	-0.1 ± 2.6	-4.0 ± 29.1
96	0.2 ± 5.0	8.3 ± 0.0	-2.9 ± 16.8	-0.8 ± 1.7	-4.4 ± 45.4

Table S2: Effective force exerted between the DNA pair in presence of 6-AuNPs at $R_{+/-} = 1.0$ corresponding to 40 AuNPs without counterions in the system.

ℓ(Å)	F/F$_o$	F$_1$/F$_o$	F$_2$/F$_o$	F$_3$/F$_o$	F$_4$/F$_o$
20	154.1 ± 1.8	310.7 ± 0.0	0.0 ± 0.0	0.0 ± 0.0	-156.6 ± 1.8
22	98.6 ± 1.4	256.6 ± 0.0	0.0 ± 0.0	0.0 ± 0.0	-158.0 ± 1.4
24	62.7 ± 1.0	229.6 ± 0.0	0.0 ± 0.0	0.0 ± 0.0	-166.9 ± 1.0
26	31.0 ± 7.0	209.5 ± 0.0	0.0 ± 0.0	0.0 ± 0.0	-178.5 ± 7.0
28	0.7 ± 1.8	192.6 ± 0.0	0.0 ± 0.0	0.0 ± 0.0	-191.9 ± 1.8
30	-10.2 ± 0.7	178.1 ± 0.0	0.0 ± 0.0	0.0 ± 0.0	-188.3 ± 0.7
32	-13.7 ± 0.3	165.2 ± 0.0	0.0 ± 0.0	0.0 ± 0.0	-178.9 ± 0.3
34	-13.1 ± 0.3	153.8 ± 0.0	0.0 ± 0.0	0.0 ± 0.0	-166.9 ± 0.3
36	-10.5 ± 0.2	143.5 ± 0.0	0.0 ± 0.0	0.0 ± 0.0	-154.0 ± 0.2
38	-6.7 ± 0.2	134.2 ± 0.0	0.0 ± 0.0	0.0 ± 0.0	-140.9 ± 0.2
40	-3.4 ± 1.0	125.7 ± 0.0	0.0 ± 0.0	0.0 ± 0.0	-129.1 ± 1.0
42	-1.8 ± 0.2	117.9 ± 0.0	0.0 ± 0.0	0.0 ± 0.0	-119.7 ± 0.2
44	-1.0 ± 0.2	110.7 ± 0.0	0.0 ± 0.0	0.0 ± 0.0	-111.7 ± 0.2
46	-1.1 ± 1.0	104.0 ± 0.0	0.0 ± 0.0	0.0 ± 0.0	-105.1 ± 1.0
48	-0.2 ± 0.6	97.8 ± 0.0	0.0 ± 0.0	0.0 ± 0.0	-98.0 ± 0.6
50	-0.1 ± 0.3	92.0 ± 0.0	0.0 ± 0.0	0.0 ± 0.0	-92.1 ± 0.3
52	0.1 ± 1.4	86.5 ± 0.0	0.0 ± 0.0	0.0 ± 0.0	-86.4 ± 1.4
54	0.3 ± 0.2	81.4 ± 0.0	0.0 ± 0.0	0.0 ± 0.0	-81.1 ± 0.2
56	-0.2 ± 0.5	76.5 ± 0.0	0.0 ± 0.0	0.0 ± 0.0	-76.7 ± 0.5
58	0.1 ± 0.5	71.9 ± 0.0	0.0 ± 0.0	0.0 ± 0.0	-71.8 ± 0.5
60	-0.1 ± 0.5	67.5 ± 0.0	0.0 ± 0.0	0.0 ± 0.0	-67.6 ± 0.5
62	-0.3 ± 0.2	63.3 ± 0.0	0.0 ± 0.0	0.0 ± 0.0	-63.6 ± 0.2
64	-0.9 ± 1.2	59.3 ± 0.0	0.0 ± 0.0	0.0 ± 0.0	-60.2 ± 1.2
66	0.0 ± 0.5	55.4 ± 0.0	0.0 ± 0.0	0.0 ± 0.0	-55.4 ± 0.5
68	0.0 ± 0.4	51.7 ± 0.0	0.0 ± 0.0	0.0 ± 0.0	-51.7 ± 0.4
70	-0.4 ± 0.3	48.1 ± 0.0	0.0 ± 0.0	0.0 ± 0.0	-48.5 ± 0.3
72	0.1 ± 0.3	44.6 ± 0.0	0.0 ± 0.0	0.0 ± 0.0	-44.5 ± 0.3
74	0.3 ± 0.1	41.2 ± 0.0	0.0 ± 0.0	0.0 ± 0.0	-40.9 ± 0.1
76	-0.2 ± 1.6	38.0 ± 0.0	0.0 ± 0.0	0.0 ± 0.0	-38.2 ± 1.6
78	0.0 ± 0.1	34.8 ± 0.0	0.0 ± 0.0	0.0 ± 0.0	-34.8 ± 0.1
80	0.0 ± 0.1	31.6 ± 0.0	0.0 ± 0.0	0.0 ± 0.0	-31.6 ± 0.1
82	0.5 ± 1.1	28.6 ± 0.0	0.0 ± 0.0	0.0 ± 0.0	-28.1 ± 1.1
84	-0.2 ± 0.2	25.5 ± 0.0	0.0 ± 0.0	0.0 ± 0.0	-25.7 ± 0.2
86	0.0 ± 0.1	22.6 ± 0.0	0.0 ± 0.0	0.0 ± 0.0	-22.6 ± 0.1
88	0.2 ± 1.0	19.7 ± 0.0	0.0 ± 0.0	0.0 ± 0.0	-19.5 ± 1.0
90	-0.1 ± 0.1	16.8 ± 0.0	0.0 ± 0.0	0.0 ± 0.0	-16.9 ± 0.1
92	0.0 ± 0.1	13.9 ± 0.0	0.0 ± 0.0	0.0 ± 0.0	-13.9 ± 0.1
94	-0.8 ± 1.0	11.1 ± 0.0	0.0 ± 0.0	0.0 ± 0.0	-11.9 ± 1.0
96	0.0 ± 0.4	8.3 ± 0.0	0.0 ± 0.0	0.0 ± 0.0	-8.3 ± 0.4

Table S3: Effective force exerted between the DNA pair in presence of 6-AuNPs at $R_{+/-} = 1.0$ corresponding to 40 AuNPs, 240 counter-cations and 240 counter-anions in the system.

ℓ(Å)	F/F$_o$	F$_1$/F$_o$	F$_2$/F$_o$	F$_3$/F$_o$	F$_4$/F$_o$
20	117.9 ± 7.4	310.7 ± 0.0	-91.2 ± 6.9	-4.8 ± 0.2	-96.8 ± 18.5
22	65.1 ± 10.5	256.6 ± 0.0	-77.5 ± 5.3	-3.9 ± 4.8	-110.1 ± 7.7
24	38.9 ± 1.7	229.6 ± 0.0	-63.0 ± 4.9	-5.4 ± 0.1	-122.3 ± 6.0
26	21.1 ± 0.7	209.5 ± 0.0	-42.3 ± 2.4	-5.3 ± 0.1	-140.8 ± 3.0
28	3.4 ± 6.0	192.6 ± 0.0	-23.8 ± 6.6	-5.6 ± 0.1	-159.8 ± 23.0
30	-9.0 ± 0.5	178.1 ± 0.0	-13.7 ± 0.5	-5.5 ± 0.2	-167.9 ± 1.3
32	-11.5 ± 0.9	165.2 ± 0.0	-13.1 ± 1.8	-5.1 ± 0.1	-158.5 ± 4.1
34	-11.2 ± 0.3	153.8 ± 0.0	-14.1 ± 1.2	-4.6 ± 0.2	-146.3 ± 1.7
36	-8.3 ± 0.5	143.5 ± 0.0	-14.7 ± 1.0	-3.8 ± 0.2	-133.3 ± 2.7
38	-4.8 ± 0.6	134.2 ± 0.0	-14.9 ± 1.2	-2.9 ± 0.4	-121.2 ± 3.0
40	-1.7 ± 0.2	125.7 ± 0.0	-15.7 ± 1.3	-2.0 ± 0.1	-109.7 ± 1.4
42	-0.4 ± 0.6	117.9 ± 0.0	-16.1 ± 0.8	-1.4 ± 0.3	-100.8 ± 1.7
44	0.9 ± 0.5	110.7 ± 0.0	-16.3 ± 2.6	-0.9 ± 0.4	-92.6 ± 6.7
46	1.3 ± 0.5	104.0 ± 0.0	-15.2 ± 0.7	-0.1 ± 0.4	-87.4 ± 1.0
48	1.2 ± 0.5	97.8 ± 0.0	-14.2 ± 1.4	0.3 ± 0.3	-82.7 ± 3.5
50	1.5 ± 0.5	92.0 ± 0.0	-13.8 ± 0.7	0.6 ± 0.9	-77.3 ± 2.6
52	1.2 ± 0.4	86.5 ± 0.0	-12.7 ± 1.2	0.8 ± 1.1	-73.4 ± 0.9
54	0.9 ± 0.5	81.4 ± 0.0	-11.5 ± 0.7	1.0 ± 0.9	-70.0 ± 3.4
56	1.0 ± 0.2	76.5 ± 0.0	-10.9 ± 1.0	1.0 ± 0.4	-65.6 ± 2.6
58	0.9 ± 0.2	71.9 ± 0.0	-10.6 ± 1.6	1.5 ± 0.5	-61.9 ± 2.7
60	0.8 ± 0.6	67.5 ± 0.0	-9.9 ± 1.3	1.5 ± 0.8	-58.3 ± 4.3
62	0.4 ± 0.3	63.3 ± 0.0	-9.0 ± 1.4	1.9 ± 0.7	-55.8 ± 2.7
64	0.4 ± 0.3	59.3 ± 0.0	-7.9 ± 0.9	1.9 ± 0.5	-52.9 ± 3.2
66	0.4 ± 0.1	55.4 ± 0.0	-6.6 ± 0.6	1.5 ± 0.5	-49.9 ± 0.5
68	0.0 ± 0.4	51.7 ± 0.0	-6.4 ± 0.7	1.3 ± 0.9	-46.6 ± 2.1
70	0.4 ± 0.3	48.1 ± 0.0	-6.0 ± 1.4	1.5 ± 1.1	-43.2 ± 1.8
72	0.4 ± 0.4	44.6 ± 0.0	-6.1 ± 1.6	1.5 ± 1.4	-39.6 ± 3.0
74	0.4 ± 1.2	41.2 ± 0.0	-6.0 ± 1.2	1.1 ± 1.4	-35.9 ± 6.9
76	0.3 ± 0.4	38.0 ± 0.0	-5.0 ± 0.7	1.5 ± 1.3	-34.2 ± 2.2
78	0.1 ± 0.3	34.8 ± 0.0	-4.3 ± 0.9	1.0 ± 0.3	-31.4 ± 2.2
80	3.2 ± 20.1	31.6 ± 0.0	-2.9 ± 1.2	0.9 ± 0.9	-26.4 ± 2.3
82	0.1 ± 0.5	28.6 ± 0.0	-3.2 ± 0.9	1.0 ± 0.7	-26.3 ± 3.5
84	0.0 ± 0.4	25.5 ± 0.0	-2.9 ± 1.7	0.8 ± 0.8	-23.4 ± 2.3
86	0.3 ± 0.5	22.6 ± 0.0	-3.3 ± 0.8	1.0 ± 0.5	-20.0 ± 2.2
88	-0.1 ± 0.5	19.7 ± 0.0	-2.2 ± 0.5	1.0 ± 0.7	-18.6 ± 1.3
90	-0.1 ± 0.3	16.8 ± 0.0	-2.1 ± 0.8	0.5 ± 1.1	-15.3 ± 2.7
92	-0.2 ± 0.7	13.9 ± 0.0	-1.5 ± 0.5	1.0 ± 2.2	-13.6 ± 5.0
94	0.1 ± 0.3	11.1 ± 0.0	-1.0 ± 1.8	0.1 ± 0.7	-10.1 ± 4.3
96	-0.4 ± 0.6	8.3 ± 0.0	0.3 ± 1.0	0.1 ± 0.4	-9.1 ± 2.7

Table S4: Effective force exerted between the DNA pair in presence of 6-AuNPs at $R_{+/-} = 1.5$ corresponding to 60 AuNPs, 240 counter-cations and 360 counter-anions in the system.

ℓ(Å)	F/F$_o$	F$_1$/F$_o$	F$_2$/F$_o$	F$_3$/F$_o$	F$_4$/F$_o$
20	119.2 ± 1.8	310.7 ± 0.0	-83.3 ± 5.3	-7.4 ± 0.0	-100.8 ± 1.4
22	67.8 ± 3.3	256.6 ± 0.0	-75.2 ± 5.9	-7.8 ± 2.0	-105.8 ± 16.5
24	42.4 ± 1.0	229.6 ± 0.0	-54.3 ± 3.2	-8.1 ± 0.1	-124.8 ± 1.4
26	24.1 ± 0.5	209.5 ± 0.0	-36.5 ± 2.2	-8.1 ± 0.2	-140.8 ± 3.7
28	3.1 ± 5.6	192.6 ± 0.0	-17.2 ± 3.7	-8.0 ± 0.3	-164.3 ± 17.6
30	-7.9 ± 0.5	178.1 ± 0.0	-10.1 ± 1.0	-7.6 ± 0.1	-168.3 ± 1.6
32	-10.9 ± 0.3	165.2 ± 0.0	-9.4 ± 0.5	-6.9 ± 0.3	-159.8 ± 1.2
34	-9.9 ± 0.1	153.8 ± 0.0	-9.6 ± 0.7	-5.7 ± 0.3	-148.4 ± 1.6
36	-7.3 ± 0.6	143.5 ± 0.0	-10.2 ± 0.8	-4.3 ± 0.4	-136.3 ± 2.2
38	-3.6 ± 0.4	134.2 ± 0.0	-11.7 ± 2.0	-3.2 ± 0.3	-122.9 ± 4.8
40	-1.0 ± 0.3	125.7 ± 0.0	-12.3 ± 1.3	-2.5 ± 0.5	-111.9 ± 2.4
42	0.6 ± 0.3	117.9 ± 0.0	-12.2 ± 0.5	-1.1 ± 0.3	-104.0 ± 0.6
44	1.8 ± 0.2	110.7 ± 0.0	-11.6 ± 1.0	-0.3 ± 1.2	-97.0 ± 2.6
46	2.0 ± 0	104.0 ± 0.0	-11.6 ± 0.6	0.7 ± 0.5	-91.1 ± 1.3
48	1.6 ± 0.3	97.8 ± 0.0	-9.8 ± 1.1	1.3 ± 0.4	-87.7 ± 1.9
50	1.8 ± 0.2	92.0 ± 0.0	-9.5 ± 0.5	1.9 ± 1.2	-82.6 ± 3.7
52	1.7 ± 0.3	86.5 ± 0.0	-8.6 ± 0.4	2.8 ± 1.5	-79.0 ± 1.5
54	1.5 ± 0.6	81.4 ± 0.0	-8.1 ± 1.0	3.5 ± 0.5	-75.3 ± 3.2
56	1.1 ± 0.5	76.5 ± 0.0	-6.6 ± 1.0	3.0 ± 0.5	-71.8 ± 1.7
58	1.0 ± 0.1	71.9 ± 0.0	-7.0 ± 1.0	2.7 ± 1.7	-66.6 ± 1.3
60	1.0 ± 0.3	67.5 ± 0.0	-6.0 ± 0.4	2.8 ± 0.9	-63.3 ± 2.5
62	0.9 ± 0.3	63.3 ± 0.0	-5.7 ± 1.4	3.6 ± 1.2	-60.3 ± 5.3
64	0.7 ± 0.4	59.3 ± 0.0	-4.7 ± 1.0	4.3 ± 1.4	-58.2 ± 5.0
66	0.3 ± 0.1	55.4 ± 0.0	-4.7 ± 0.7	3.6 ± 1.4	-54.0 ± 2.1
68	0.3 ± 0.1	51.7 ± 0.0	-3.6 ± 1.4	3.8 ± 1.0	-51.6 ± 2.6
70	0.4 ± 0.2	48.1 ± 0.0	-3.7 ± 0.6	3.2 ± 2.2	-47.2 ± 3.1
72	0.1 ± 0.2	44.6 ± 0.0	-2.5 ± 1.3	2.6 ± 1.8	-44.6 ± 3.6
74	-0.1 ± 0.2	41.2 ± 0.0	-2.6 ± 0.5	2.5 ± 1.4	-41.2 ± 2.3
76	0.4 ± 0.2	38.0 ± 0.0	-2.3 ± 1.4	2.9 ± 1.8	-38.2 ± 4.1
78	0.1 ± 0.7	34.8 ± 0.0	-1.5 ± 0.6	2.7 ± 1.0	-35.9 ± 5.0
80	0.0 ± 0.2	31.6 ± 0.0	-2.7 ± 0.6	2.4 ± 1.2	-31.3 ± 2.7
82	0.1 ± 0.2	28.6 ± 0.0	-1.7 ± 1.1	2.2 ± 0.7	-29.0 ± 2.9
84	0.0 ± 0.5	25.5 ± 0.0	-1.1 ± 0.6	1.2 ± 1.5	-25.6 ± 1.8
86	-0.3 ± 0.3	22.6 ± 0.0	-1.0 ± 1.6	1.2 ± 0.8	-23.1 ± 3.0
88	-0.2 ± 0.3	19.7 ± 0.0	-1.4 ± 1.7	1.2 ± 2.1	-19.7 ± 3.2
90	0.1 ± 0.4	16.8 ± 0.0	-1.3 ± 1.4	0.8 ± 0.6	-16.2 ± 2.2
92	-0.1 ± 0.3	13.9 ± 0.0	-1.4 ± 0.8	0.8 ± 0.8	-13.4 ± 2.3
94	0.0 ± 0.4	11.1 ± 0.0	-0.5 ± 1.5	0.1 ± 0.4	-10.7 ± 4.3
96	0.1 ± 0.1	8.3 ± 0.0	-0.3 ± 0.4	0.2 ± 0.9	-8.1 ± 0.3

Table S5: Effective force exerted between the DNA pair in presence of 12-AuNPs at $R_{+/-} = 0.5$ corresponding to 10 AuNPs, 240 counter-cations and 120 counter-anions in the system.

ℓ(Å)	F/F$_o$	F$_1$/F$_o$	F$_2$/F$_o$	F$_3$/F$_o$	F$_4$/F$_o$
20	68.0 ± 27.1	310.7 ± 0.0	-84.0 ± 66.5	-1.6 ± 0.1	-157.1 ± 181.5
22	13.9 ± 44.3	256.6 ± 0.0	-71.1 ± 87.5	-1.6 ± 0.3	-170.0 ± 269.6
24	-8.8 ± 63.4	229.6 ± 0.0	-56.7 ± 128.6	-2.0 ± 0.4	-179.7 ± 393.2
26	-24.2 ± 119.3	209.5 ± 0.0	-41.7 ± 191.7	-2.1 ± 0.4	-189.9 ± 641.1
28	-38.0 ± 59.5	192.6 ± 0.0	-25.5 ± 67.5	-2.8 ± 0.3	-202.3 ± 262.0
30	-52.1 ± 114.9	178.1 ± 0.0	-15.3 ± 101.8	-3.2 ± 0.3	-211.7 ± 444.3
32	-40.5 ± 98.5	165.2 ± 0.0	-20.9 ± 95.8	-4.3 ± 0.4	-180.5 ± 400.6
34	-39.0 ± 99.7	153.8 ± 0.0	-18.7 ± 73.3	-4.4 ± 0.5	-169.7 ± 363.5
36	-35.6 ± 112.1	143.5 ± 0.0	-18.6 ± 89.4	-4.2 ± 0.6	-156.3 ± 428.7
38	-35.0 ± 35.2	134.2 ± 0.0	-14.5 ± 24.8	-3.2 ± 0.7	-151.5 ± 134.5
40	-22.8 ± 18.5	125.7 ± 0.0	-21.7 ± 25.2	-3.6 ± 0.6	-123.2 ± 93.7
42	-19.8 ± 27.3	117.9 ± 0.0	-22.4 ± 27.4	-2.4 ± 0.7	-112.9 ± 122.5
44	-15.5 ± 24.2	110.7 ± 0.0	-25.8 ± 26.7	-2.1 ± 0.4	-98.3 ± 111.6
46	-8.1 ± 15.7	104.0 ± 0.0	-32.8 ± 21.7	-2.4 ± 0.6	-76.9 ± 84.0
48	-11.1 ± 16.1	97.8 ± 0.0	-28.2 ± 26.5	-1.5 ± 0.7	-79.2 ± 94.3
50	-6.7 ± 10.3	92.0 ± 0.0	-31.5 ± 11.5	-2.1 ± 0.3	-65.1 ± 47.8
52	-7.0 ± 18.1	86.5 ± 0.0	-29.2 ± 24.8	-1.7 ± 0.8	-62.6 ± 99.0
54	-4.8 ± 13.8	81.4 ± 0.0	-29.8 ± 20.0	-1.7 ± 0.3	-54.7 ± 74.1
56	-3.9 ± 36.1	76.5 ± 0.0	-28.5 ± 43.5	-2.1 ± 1.1	-49.8 ± 183.7
58	-1.5 ± 34.5	71.9 ± 0.0	-29.6 ± 40.7	-2.0 ± 1.1	-41.8 ± 175.4
60	-3.6 ± 19.9	67.5 ± 0.0	-25.7 ± 23.9	-1.3 ± 1.0	-44.1 ± 103.6
62	-3.3 ± 15.5	63.3 ± 0.0	-24.6 ± 18.2	-1.1 ± 0.8	-40.9 ± 74.1
64	-1.0 ± 12.6	59.3 ± 0.0	-25.7 ± 17.7	-1.3 ± 0.5	-33.3 ± 66.2
66	-2.4 ± 17.2	55.4 ± 0.0	-22.9 ± 17.4	-1.3 ± 1.0	-33.6 ± 84.5
68	-5.9 ± 46.4	51.7 ± 0.0	-17.6 ± 52.7	-0.7 ± 2.5	-39.3 ± 238.0
70	-0.8 ± 22.0	48.1 ± 0.0	-21.0 ± 19.9	-1.3 ± 1.8	-26.6 ± 104.9
72	-0.8 ± 34.8	44.6 ± 0.0	-19.5 ± 37.1	-1.5 ± 0.9	-24.4 ± 160.8
74	-2.3 ± 17.2	41.2 ± 0.0	-16.4 ± 18.3	-0.6 ± 1.2	-26.5 ± 87.8
76	-0.3 ± 16.2	38.0 ± 0.0	-17.1 ± 15.3	-0.8 ± 0.7	-20.4 ± 72.6
78	-2.8 ± 45.6	34.8 ± 0.0	-13.1 ± 48.0	-0.5 ± 2.1	-24.0 ± 222.2
80	-0.9 ± 27.7	31.6 ± 0.0	-13.5 ± 34.3	-1.1 ± 2.1	-17.9 ± 144.5
82	0.4 ± 20.7	28.6 ± 0.0	-13.5 ± 21.4	-1.2 ± 1.2	-13.5 ± 102.8
84	0.5 ± 26.9	25.5 ± 0.0	-12.4 ± 31.1	-1.2 ± 1.3	-11.4 ± 138.6
86	-0.9 ± 23.7	22.6 ± 0.0	-9.7 ± 25.2	-0.5 ± 0.4	-13.3 ± 107.8
88	-1.4 ± 47.1	19.7 ± 0.0	-7.8 ± 40.1	-0.7 ± 3.6	-12.6 ± 223.9
90	-4.1 ± 26.0	16.8 ± 0.0	-3.4 ± 29.4	0.3 ± 1.9	-17.8 ± 135.3
92	-1.5 ± 13.4	13.9 ± 0.0	-5.4 ± 17.3	0.0 ± 0.4	-10.0 ± 68.1
94	-0.1 ± 34.7	11.1 ± 0.0	-4.6 ± 31.5	-0.5 ± 2.5	-6.1 ± 167.5
96	0.9 ± 19.8	8.3 ± 0.0	-4.6 ± 20.7	-0.5 ± 0.7	-2.3 ± 91.0

Table S6: Effective force exerted between the DNA pair in presence of 12-AuNPs at $R_{+/-} = 1.0$ corresponding to 20 AuNPs without counterions in the system.

ℓ(Å)	F/F$_o$	F$_1$/F$_o$	F$_2$/F$_o$	F$_3$/F$_o$	F$_4$/F$_o$
20	127.0 ± 209.8	310.7 ± 0.0	0.0 ± 0.0	0.0 ± 0.0	-183.7 ± 209.8
22	60.9 ± 291.3	256.6 ± 0.0	0.0 ± 0.0	0.0 ± 0.0	-195.7 ± 291.3
24	15.1 ± 298.1	229.6 ± 0.0	0.0 ± 0.0	0.0 ± 0.0	-214.5 ± 298.1
26	-6.9 ± 178.9	209.5 ± 0.0	0.0 ± 0.0	0.0 ± 0.0	-216.4 ± 178.9
28	-37.1 ± 101.9	192.6 ± 0.0	0.0 ± 0.0	0.0 ± 0.0	-229.7 ± 101.9
30	-62.1 ± 15.4	178.1 ± 0.0	0.0 ± 0.0	0.0 ± 0.0	-240.2 ± 15.4
32	-32.6 ± 45.7	165.2 ± 0.0	0.0 ± 0.0	0.0 ± 0.0	-197.8 ± 45.7
34	-11.4 ± 74.8	153.8 ± 0.0	0.0 ± 0.0	0.0 ± 0.0	-165.2 ± 74.8
36	-7.0 ± 17.5	143.5 ± 0.0	0.0 ± 0.0	0.0 ± 0.0	-150.5 ± 17.5
38	-0.2 ± 16.7	134.2 ± 0.0	0.0 ± 0.0	0.0 ± 0.0	-134.4 ± 16.7
40	5.4 ± 25.2	125.7 ± 0.0	0.0 ± 0.0	0.0 ± 0.0	-120.3 ± 25.2
42	3.3 ± 30.2	117.9 ± 0.0	0.0 ± 0.0	0.0 ± 0.0	-114.6 ± 30.2
44	1.9 ± 14.3	110.7 ± 0.0	0.0 ± 0.0	0.0 ± 0.0	-108.8 ± 14.3
46	1.6 ± 24.7	104.0 ± 0.0	0.0 ± 0.0	0.0 ± 0.0	-102.4 ± 24.7
48	3.5 ± 50.5	97.8 ± 0.0	0.0 ± 0.0	0.0 ± 0.0	-94.3 ± 50.5
50	3.7 ± 15.2	92.0 ± 0.0	0.0 ± 0.0	0.0 ± 0.0	-88.3 ± 15.2
52	2.3 ± 27.6	86.5 ± 0.0	0.0 ± 0.0	0.0 ± 0.0	-84.2 ± 27.6
54	5.5 ± 30.7	81.4 ± 0.0	0.0 ± 0.0	0.0 ± 0.0	-75.9 ± 30.7
56	2.1 ± 33.3	76.5 ± 0.0	0.0 ± 0.0	0.0 ± 0.0	-74.4 ± 33.3
58	5.4 ± 15	71.9 ± 0.0	0.0 ± 0.0	0.0 ± 0.0	-66.5 ± 15.0
60	4.4 ± 47.5	67.5 ± 0.0	0.0 ± 0.0	0.0 ± 0.0	-63.1 ± 47.5
62	0.2 ± 14.8	63.3 ± 0.0	0.0 ± 0.0	0.0 ± 0.0	-63.1 ± 14.8
64	2.0 ± 33.9	59.3 ± 0.0	0.0 ± 0.0	0.0 ± 0.0	-57.3 ± 33.9
66	1.5 ± 50.0	55.4 ± 0.0	0.0 ± 0.0	0.0 ± 0.0	-53.9 ± 50.0
68	0.7 ± 18.3	51.7 ± 0.0	0.0 ± 0.0	0.0 ± 0.0	-51.0 ± 18.3
70	-2.9 ± 25.7	48.1 ± 0.0	0.0 ± 0.0	0.0 ± 0.0	-51.0 ± 25.7
72	-1.3 ± 21.8	44.6 ± 0.0	0.0 ± 0.0	0.0 ± 0.0	-45.9 ± 21.8
74	-0.5 ± 7.6	41.2 ± 0.0	0.0 ± 0.0	0.0 ± 0.0	-41.7 ± 7.6
76	1.0 ± 31.0	38.0 ± 0.0	0.0 ± 0.0	0.0 ± 0.0	-37.0 ± 31.0
78	-0.9 ± 11.2	34.8 ± 0.0	0.0 ± 0.0	0.0 ± 0.0	-35.7 ± 11.2
80	1.1 ± 20.0	31.6 ± 0.0	0.0 ± 0.0	0.0 ± 0.0	-30.5 ± 20.0
82	-0.8 ± 21.3	28.6 ± 0.0	0.0 ± 0.0	0.0 ± 0.0	-29.4 ± 21.3
84	1.0 ± 16.6	25.5 ± 0.0	0.0 ± 0.0	0.0 ± 0.0	-24.5 ± 16.6
86	0.8 ± 17.3	22.6 ± 0.0	0.0 ± 0.0	0.0 ± 0.0	-21.8 ± 17.3
88	-0.9 ± 22.3	19.7 ± 0.0	0.0 ± 0.0	0.0 ± 0.0	-20.6 ± 22.3
90	-0.3 ± 10.2	16.8 ± 0.0	0.0 ± 0.0	0.0 ± 0.0	-17.1 ± 10.2
92	-0.6 ± 14.1	13.9 ± 0.0	0.0 ± 0.0	0.0 ± 0.0	-14.5 ± 14.1
94	1.4 ± 70.1	11.1 ± 0.0	0.0 ± 0.0	0.0 ± 0.0	-9.7 ± 70.1
96	0.9 ± 21.1	8.3 ± 0.0	0.0 ± 0.0	0.0 ± 0.0	-7.4 ± 21.1

Table S7: Effective force exerted between the DNA pair in presence of 12-AuNPs at $R_{+/-} = 1.0$ corresponding to 20 AuNPs, 240 counter-cations and 240 counter-anions in the system.

ℓ(Å)	F/F$_o$	F$_1$/F$_o$	F$_2$/F$_o$	F$_3$/F$_o$	F$_4$/F$_o$
20	92.8 ± 34.9	310.7 ± 0.0	-38.8 ± 25.3	-2.6 ± 2.4	-176.5 ± 115.8
22	43.3 ± 37.4	256.6 ± 0.0	-31.9 ± 29.1	-4.3 ± 2.3	-177.1 ± 143.6
24	13.8 ± 33.0	229.6 ± 0.0	-18.0 ± 9.4	-4.3 ± 2.2	-193.5 ± 98.6
26	-5.5 ± 1.7	209.5 ± 0.0	-9.6 ± 3.9	-4.6 ± 0.2	-200.8 ± 7.6
28	-31.5 ± 87.8	192.6 ± 0.0	-0.1 ± 22.0	-3.0 ± 5.6	-221.0 ± 251.2
30	-35.3 ± 148.6	178.1 ± 0.0	-3.3 ± 37.4	-3.9 ± 8.8	-206.2 ± 446.3
32	-21.8 ± 41.1	165.2 ± 0.0	-9.2 ± 8.6	-6.8 ± 2.4	-171.0 ± 111.8
34	-15.8 ± 17.5	153.8 ± 0.0	-10.5 ± 2.7	-7.6 ± 1.6	-151.5 ± 46.0
36	-14.3 ± 18.7	143.5 ± 0.0	-9.8 ± 7.4	-5.1 ± 1.7	-142.9 ± 66.2
38	-6.0 ± 4.9	134.2 ± 0.0	-12.0 ± 1.0	-3.6 ± 2.8	-124.6 ± 18.1
40	0.5 ± 8.2	125.7 ± 0.0	-14.1 ± 2.6	-1.6 ± 3.1	-109.5 ± 34.1
42	4.1 ± 4.4	117.9 ± 0.0	-14.8 ± 1.7	0.6 ± 0.9	-99.6 ± 16.1
44	2.6 ± 8.4	110.7 ± 0.0	-14.1 ± 2.9	3.1 ± 3.1	-97.1 ± 35.9
46	4.3 ± 2.0	104.0 ± 0.0	-15.3 ± 3.6	3.5 ± 1.8	-87.9 ± 14.3
48	4.5 ± 3.5	97.8 ± 0.0	-15.2 ± 2.9	4.0 ± 2.1	-82.1 ± 20.3
50	4.5 ± 3.7	92.0 ± 0.0	-14.7 ± 4.3	3.5 ± 2.0	-76.3 ± 22.7
52	1.5 ± 11.0	86.5 ± 0.0	-11.9 ± 9.1	5.9 ± 2.4	-79.0 ± 55.8
54	4.3 ± 4.2	81.4 ± 0.0	-12.9 ± 5.6	4.7 ± 1.5	-68.9 ± 26.4
56	2.9 ± 6.7	76.5 ± 0.0	-12.2 ± 3.3	5.2 ± 3.0	-66.6 ± 30.1
58	2.9 ± 3.0	71.9 ± 0.0	-10.8 ± 1.8	4.6 ± 1.1	-62.8 ± 8.1
60	2.0 ± 4.3	67.5 ± 0.0	-10.6 ± 3.8	5.3 ± 2.1	-60.2 ± 23.9
62	1.1 ± 13.8	63.3 ± 0.0	-8.8 ± 5.5	5.7 ± 5.0	-59.1 ± 61.1
64	2.8 ± 12.2	59.3 ± 0.0	-9.2 ± 7.3	4.9 ± 3.8	-52.2 ± 60.1
66	1.3 ± 6.6	55.4 ± 0.0	-8.1 ± 4.6	4.9 ± 1.7	-50.9 ± 30.1
68	3.8 ± 9.0	51.7 ± 0.0	-8.8 ± 8.8	3.3 ± 2.6	-42.4 ± 40.8
70	1.9 ± 7.4	48.1 ± 0.0	-8.0 ± 8.0	4.2 ± 1.0	-42.4 ± 35.8
72	1.7 ± 5.0	44.6 ± 0.0	-6.3 ± 2.5	3.5 ± 2.5	-40.1 ± 18.9
74	0.7 ± 5.1	41.2 ± 0.0	-5.7 ± 1.7	4.3 ± 1.8	-39.1 ± 19.1
76	1.1 ± 21.3	38.0 ± 0.0	-5.3 ± 18.6	3.5 ± 4.9	-35.1 ± 19.0
78	1.7 ± 16.0	34.8 ± 0.0	-5.7 ± 14.4	3.3 ± 1.2	-30.7 ± 19.2
80	-0.2 ± 4.7	31.6 ± 0.0	-3.5 ± 3.7	3.3 ± 1.7	-31.6 ± 22.7
82	-0.4 ± 2.8	28.6 ± 0.0	-3.0 ± 3.0	3.3 ± 0.4	-29.3 ± 9.6
84	1.4 ± 6.6	25.5 ± 0.0	-4.3 ± 5.0	2.5 ± 2.5	-22.3 ± 30.7
86	2.2 ± 6.4	22.6 ± 0.0	-4.9 ± 5.1	2.4 ± 0.8	-17.9 ± 28.6
88	0.9 ± 18.3	19.7 ± 0.0	-3.2 ± 18.4	1.5 ± 2.1	-17.1 ± 97.1
90	1.1 ± 6.0	16.8 ± 0.0	-3.6 ± 3.5	2.1 ± 1.2	-14.2 ± 23.2
92	1.3 ± 7.8	13.9 ± 0.0	-2.9 ± 5.9	1.2 ± 2.1	-10.9 ± 38.1
94	-0.7 ± 1.9	11.1 ± 0.0	-0.7 ± 0.6	1.7 ± 1.2	-12.8 ± 7.0
96	1.2 ± 11.2	8.3 ± 0.0	-2.3 ± 10.2	0.1 ± 2.1	-4.9 ± 27.6

Table S8: Effective force exerted between the DNA pair in presence of 12-AuNPs at $R_{+/-} = 1.5$ corresponding to 30 AuNPs, 240 counter-cations and 360 counter-anions in the system.

ℓ(Å)	F/F$_o$	F$_1$/F$_o$	F$_2$/F$_o$	F$_3$/F$_o$	F$_4$/F$_o$
20	117.6 ± 28.5	310.7 ± 0.0	-22.2 ± 28.6	-1.7 ± 5.6	-169.2 ± 157.1
22	57.4 ± 14.8	256.6 ± 0.0	-13.9 ± 4.9	-2.0 ± 2.6	-183.3 ± 49.1
24	19.7 ± 52.9	229.6 ± 0.0	-3.8 ± 5.8	1.3 ± 7.8	-207.4 ± 148.4
26	-2.5 ± 92.2	209.5 ± 0.0	0.9 ± 4.1	2.3 ± 14.6	-215.2 ± 234.2
28	-15.6 ± 33.2	192.6 ± 0.0	3.3 ± 0.7	4.2 ± 13.2	-215.7 ± 100.5
30	-21.9 ± 7.1	178.1 ± 0.0	3.7 ± 0.8	6.1 ± 4.7	-209.8 ± 25.3
32	-16.0 ± 12.0	165.2 ± 0.0	2.8 ± 0.3	7.5 ± 2.1	-191.5 ± 23.0
34	-10.7 ± 3.1	153.8 ± 0.0	2.4 ± 0.3	8.4 ± 1.5	-175.3 ± 8.6
36	-6.3 ± 3.5	143.5 ± 0.0	2.1 ± 0.4	11.2 ± 3.6	-163.1 ± 13.8
38	-0.6 ± 1.6	134.2 ± 0.0	1.8 ± 0.5	15.0 ± 3.6	-151.6 ± 8.5
40	3.9 ± 1.2	125.7 ± 0.0	1.0 ± 0.6	18.7 ± 4.3	-141.5 ± 14.0
42	8.5 ± 0.8	117.9 ± 0.0	0.6 ± 0.3	22.2 ± 2.6	-132.2 ± 7.1
44	9.3 ± 2.4	110.7 ± 0.0	0.2 ± 0.4	23.2 ± 1.6	-124.8 ± 9.9
46	7.6 ± 1.9	104.0 ± 0.0	0.6 ± 0.6	24.6 ± 2.4	-121.6 ± 10.6
48	7.2 ± 3.6	97.8 ± 0.0	1.2 ± 1.4	25.5 ± 2.5	-117.3 ± 19.0
50	7.0 ± 1.4	92.0 ± 0.0	1.1 ± 0.6	25.4 ± 1.3	-111.5 ± 7.4
52	5.8 ± 3.3	86.5 ± 0.0	1.8 ± 0.4	25.4 ± 2.2	-107.9 ± 13.6
54	5.0 ± 2.2	81.4 ± 0.0	2.0 ± 0.6	25.3 ± 2.2	-103.7 ± 9.8
56	2.9 ± 2.5	76.5 ± 0.0	2.6 ± 0.4	24.7 ± 1.1	-100.9 ± 7.4
58	4.2 ± 1.7	71.9 ± 0.0	2.3 ± 0.4	23.4 ± 0.5	-93.4 ± 5.6
60	3.5 ± 5.2	67.5 ± 0.0	2.5 ± 0.8	22.4 ± 2.5	-88.9 ± 20.8
62	2.4 ± 2.4	63.3 ± 0.0	2.8 ± 0.1	22.1 ± 1.0	-85.8 ± 7.0
64	2.3 ± 3.7	59.3 ± 0.0	2.6 ± 0.7	20.8 ± 2.3	-80.4 ± 16.4
66	2.5 ± 1.4	55.4 ± 0.0	2.7 ± 0.2	19.3 ± 0.6	-74.9 ± 5.0
68	0.8 ± 1.5	51.7 ± 0.0	3.2 ± 0.2	18.7 ± 0.4	-72.8 ± 4.9
70	1.5 ± 3.2	48.1 ± 0.0	2.7 ± 0.6	17.8 ± 1.0	-67.1 ± 10.3
72	1.4 ± 2.2	44.6 ± 0.0	2.9 ± 0.2	16.3 ± 0.7	-62.4 ± 6.5
74	0.9 ± 3.5	41.2 ± 0.0	2.7 ± 0.5	15.6 ± 1.8	-58.6 ± 14.9
76	1.1 ± 2.3	38.0 ± 0.0	2.7 ± 0.3	13.7 ± 0.7	-53.3 ± 7.0
78	0.8 ± 1.6	34.8 ± 0.0	2.6 ± 0.3	12.9 ± 1.2	-49.5 ± 7.6
80	0.8 ± 1.9	31.6 ± 0.0	2.4 ± 0.5	11.7 ± 1.2	-44.9 ± 9.2
82	0.3 ± 2.9	28.6 ± 0.0	2.3 ± 0.6	10.8 ± 1.1	-41.4 ± 11.1
84	0.0 ± 4.4	25.5 ± 0.0	2.2 ± 0.8	9.8 ± 1.4	-37.5 ± 14.7
86	0.8 ± 1.8	22.6 ± 0.0	1.8 ± 0.3	8.5 ± 0.6	-32.1 ± 5.5
88	-0.3 ± 2.8	19.7 ± 0.0	2.0 ± 0.2	7.6 ± 0.8	-29.6 ± 8.7
90	1.1 ± 1.3	16.8 ± 0.0	1.1 ± 0.2	6.0 ± 0.8	-22.8 ± 5.2
92	-0.3 ± 1.2	13.9 ± 0.0	1.3 ± 0.2	5.6 ± 1.2	-21.1 ± 5.7
94	-0.2 ± 1.2	11.1 ± 0.0	1.1 ± 0.3	4.2 ± 0.7	-16.6 ± 5.4
96	-0.4 ± 3.8	8.3 ± 0.0	1.0 ± 0.5	3.4 ± 0.9	-13.1 ± 12.3

S6 Numerical tests of our MC simulation package

Our MC simulation package presented in section S3 is set up in order to insert or remove a pair of positive and negative ions (i.e., a ion salt pair) to perform Grand Canonical Monte Carlo (GCMC) simulations used to compute the osmotic pressure in the supernatant phase (see Section 3.3 of the main text). In order to validate our implementation of the MC simulation package, we perform simulations on simple systems of solution of monovalent salt by using the same interaction potential referenced in Section 2 of the main text. The validation of our MC simulation package involves two steps.

- First, we extract the excess chemical potential by using the Widom technique from a standard NVT MC simulation of an aqueous solution of constant number of monovalent salt ions. We remind that the chemical potential is expressed as the sum of two terms:[2]

$$\mu = \mu_{id} + \mu_{ex} \tag{44}$$

where μ_{id} is the contribution from "the perfect gas" to the chemical potential, which can be computed analytically and μ_{ex} is the excess part of the chemical potential that needs to be calculated with a canonical MC simulation and defined as follows:

$$\mu_{ex} = -k_B T \ln \int d\mathbf{s}^{N+1} \langle \exp[-\beta \Delta \mathcal{U}] \rangle_N \tag{45}$$

where the term $\langle \exp[-\beta \Delta \mathcal{U}] \rangle_N$ is the canonical average over configurations for the system with N salt pairs and $\Delta \mathcal{U}$ is the difference between the potential energy of the system with N+1 salt pairs and the system with N salt pairs.

Table S9: The number of ion pairs during NVT MC simulation is presented with μ_{ex} calculated using Widom insertion technique.

salt pairs (NVT)	μ_{ex} (kJ/mol)
6	-1.2988 (+/- 0.2445)
12	-1.5826 (+/- 0.3157)
24	-1.9705 (+/- 0.3984)
48	-2.4364 (+/- 0.4833)

In an orthorombic simulation box, we performed a series of NVT MC simulations for systems containing either 6, 12, 24 or 48 ion salt pairs with a diameter $d_+ = d_- = 3$ Å. The volume of the box is set to $V = (48 \text{ Å}) \times (41.57 \text{ Å}) \times (102 \text{ Å})$ and the simulation is performed for 2×10^5 MC cycles. The excess of energy is calculated every cycle to have a fair approximation of μ_{ex}. The results are presented in Table S9.

- Therein, we used the excess chemical potential μ_{ex} to calculate the total chemical potential μ and perform GCMC simulations for 2×10^5 MC cycles. We kept the same orthorombic box and for each system, there is 48 salt pairs present at the beginning of the simulation. We set the GCMC scheme such that there is the same probability to add/delete a salt pair or to displace an ion in the box. After equilibration of each system and insertion/deletion of ion pairs during the simulation, the average number of salt pairs in the box when each system is equilibrated is presented in Table S10.

Table S10: Comparison between the number of salt pairs during NVT MC simulations and the number of salt pairs in GCMC simulations for which the chemical potential has been calculated from the NVT MC simulations.

salt pairs (NVT)	salt pairs (μVT)
6	6.03 (+/- 2.61)
12	11.97 (+/- 3.84)
24	23.96 (+/- 4.46)
48	48.31 (+/- 8.35)

We found similar average number of salt pairs for both cases which validates our implementation of the MC software used in our work.

S7 Esimation of error for osmotic pressure calculations

We determined the error associated with the calculation of osmotic pressure in a hexagonal DNA lattice condensed with AuNPs. The mechanical stability of the bundle is given by the difference of osmotic pressure in the bundle and in the supernatant phase:

$$\Pi_{rel} \;=\; \Pi_{bundle} \;-\; \Pi_{bulk} \tag{46}$$

We explicit the error of Π_{bundle} and Π_{nulk} below. Given that plenty of osmotic pressure calculations has been performed, we display only the error for osmotic pressure calculations in a hexagonal lattice of DNA condensed with $\times$40 6-AuNP at constant salt concentration c_{salt} = 0, 30, 60 or 120 mM.

Table S11: Osmotic pressure in a hexagonal lattice of DNA/6-AuNPs (c_{salt} = 0 mM).

ℓ(Å)	Π_{rel} (atm.)	Π_{bundle} (atm.)	$\Pi_{supernatant}$ (atm.)
32	(-7.888 ± 0.225)	(-7.888 ± 0.225)	(0.000 ± 0.000)
40	(-3.188 ± 0.153)	(-3.188 ± 0.153)	(0.000 ± 0.000)
48	(-1.440 ± 0.131)	(-1.440 ± 0.131)	(0.000 ± 0.000)
56	(-0.779 ± 0.104)	(-0.779 ± 0.104)	(0.000 ± 0.000)
60	(-0.581 ± 0.093)	(-0.581 ± 0.093)	(0.000 ± 0.000)
62	(-0.526 ± 0.087)	(-0.526 ± 0.087)	(0.000 ± 0.000)
66	(-0.393 ± 0.079)	(-0.393 ± 0.079)	(0.000 ± 0.000)
70	(-0.302 ± 0.071)	(-0.302 ± 0.071)	(0.000 ± 0.000)
74	(-0.206 ± 0.064)	(-0.206 ± 0.064)	(0.000 ± 0.000)
78	(-0.134 ± 0.065)	(-0.134 ± 0.065)	(0.000 ± 0.000)
82	(-0.106 ± 0.053)	(-0.106 ± 0.053)	(0.000 ± 0.000)
86	(-0.071 ± 0.050)	(-0.071 ± 0.050)	(0.000 ± 0.000)
90	(-0.073 ± 0.047)	(-0.073 ± 0.047)	(0.000 ± 0.000)
94	(-0.042 ± 0.043)	(-0.042 ± 0.043)	(0.000 ± 0.000)
98	(-0.012 ± 0.039)	(-0.012 ± 0.039)	(0.000 ± 0.000)
102	(-0.018 ± 0.037)	(-0.018 ± 0.037)	(0.000 ± 0.000)

Table S12: Osmotic pressure in a hexagonal lattice of DNA/6-AuNPs (c_{salt} = 30 mM).

ℓ(Å)	Π_{rel} (atm.)	Π_{bundle} (atm.)	$\Pi_{supernatant}$ (atm.)
32	(-6.721 ± 0.302)	(-6.157 ± 0.029)	(0.563 ± 0.273)
36	(-2.848 ± 0.224)	(-2.440 ± 0.028)	(0.408 ± 0.196)
40	(-1.056 ± 0.177)	(-0.745 ± 0.028)	(0.311 ± 0.149)
44	(-0.126 ± 0.158)	(0.148 ± 0.026)	(0.275 ± 0.132)
48	(0.119 ± 0.148)	(0.382 ± 0.022)	(0.262 ± 0.126)
52	(0.321 ± 0.147)	(0.592 ± 0.019)	(0.271 ± 0.128)
54	(0.368 ± 0.144)	(0.640 ± 0.017)	(0.271 ± 0.127)
58	(0.457 ± 0.147)	(0.752 ± 0.015)	(0.294 ± 0.132)
62	(0.520 ± 0.146)	(0.842 ± 0.012)	(0.321 ± 0.134)
66	(0.548 ± 0.146)	(0.902 ± 0.011)	(0.353 ± 0.135)
70	(0.572 ± 0.149)	(0.977 ± 0.010)	(0.405 ± 0.139)
74	(0.580 ± 0.145)	(1.019 ± 0.008)	(0.439 ± 0.137)
78	(0.578 ± 0.146)	(1.067 ± 0.008)	(0.489 ± 0.138)
82	(0.584 ± 0.144)	(1.114 ± 0.007)	(0.530 ± 0.137)
86	(0.590 ± 0.142)	(1.173 ± 0.006)	(0.582 ± 0.136)
90	(0.580 ± 0.140)	(1.194 ± 0.006)	(0.614 ± 0.134)
94	(0.552 ± 0.140)	(1.225 ± 0.005)	(0.673 ± 0.135)
98	(0.544 ± 0.137)	(1.249 ± 0.005)	(0.705 ± 0.132)
102	(0.531 ± 0.135)	(1.269 ± 0.005)	(0.737 ± 0.130)

Table S13: Osmotic pressure in a hexagonal lattice of DNA/6-AuNPs (c_{salt} = 60 mM).

ℓ(Å)	Π_{rel} (atm.)	Π_{bundle} (atm.)	$\Pi_{supernatant}$ (atm.)
32	(-6.057 ± 0.759)	(-5.044 ± 0.309)	(1.012 ± 0.450)
36	(-2.178 ± 0.605)	(-1.509 ± 0.295)	(0.668 ± 0.310)
40	(-0.054 ± 0.521)	(0.451 ± 0.284)	(0.506 ± 0.237)
44	(0.624 ± 0.474)	(1.089 ± 0.261)	(0.464 ± 0.213)
48	(0.931 ± 0.434)	(1.423 ± 0.223)	(0.491 ± 0.211)
52	(1.066 ± 0.407)	(1.610 ± 0.194)	(0.543 ± 0.213)
54	(1.136 ± 0.388)	(1.714 ± 0.175)	(0.578 ± 0.213)
58	(1.155 ± 0.362)	(1.808 ± 0.149)	(0.653 ± 0.213)
62	(1.191 ± 0.351)	(1.954 ± 0.134)	(0.763 ± 0.217)
66	(1.191 ± 0.333)	(2.039 ± 0.118)	(0.848 ± 0.215)
70	(1.169 ± 0.320)	(2.126 ± 0.104)	(0.956 ± 0.216)
74	(1.138 ± 0.307)	(2.193 ± 0.092)	(1.054 ± 0.215)
78	(1.107 ± 0.301)	(2.267 ± 0.086)	(1.160 ± 0.215)
82	(1.067 ± 0.290)	(2.318 ± 0.078)	(1.250 ± 0.212)
86	(1.026 ± 0.283)	(2.380 ± 0.072)	(1.354 ± 0.211)
90	(0.985 ± 0.275)	(2.426 ± 0.067)	(1.440 ± 0.208)
94	(0.955 ± 0.266)	(2.453 ± 0.063)	(1.498 ± 0.203)
98	(0.914 ± 0.257)	(2.489 ± 0.058)	(1.575 ± 0.199)
102	(0.874 ± 0.252)	(2.513 ± 0.055)	(1.638 ± 0.197)

Table S14: Osmotic pressure in a hexagonal lattice of DNA/6-AuNPs (c_{salt} = 120 mM).

ℓ(Å)	Π_{rel} (atm.)	Π_{bundle} (atm.)	$\Pi_{supernatant}$ (atm.)
32	(-5.020 ± 1.027)	(-2.997 ± 0.339)	(2.022 ± 0.688)
36	(-0.939 ± 0.825)	(0.500 ± 0.312)	(1.440 ± 0.513)
40	(1.218 ± 0.688)	(2.307 ± 0.289)	(1.089 ± 0.399)
44	(1.996 ± 0.625)	(3.082 ± 0.262)	(1.085 ± 0.363)
48	(2.253 ± 0.573)	(3.429 ± 0.224)	(1.176 ± 0.349)
52	(2.381 ± 0.546)	(3.747 ± 0.197)	(1.365 ± 0.349)
54	(2.385 ± 0.526)	(3.842 ± 0.180)	(1.456 ± 0.346)
58	(2.350 ± 0.506)	(4.013 ± 0.159)	(1.662 ± 0.347)
62	(2.298 ± 0.489)	(4.220 ± 0.138)	(1.922 ± 0.351)
66	(2.210 ± 0.472)	(4.351 ± 0.125)	(2.141 ± 0.347)
70	(2.091 ± 0.456)	(4.476 ± 0.112)	(2.384 ± 0.344)
74	(1.994 ± 0.442)	(4.554 ± 0.101)	(2.559 ± 0.341)
78	(1.921 ± 0.429)	(4.666 ± 0.094)	(2.745 ± 0.335)
82	(1.801 ± 0.415)	(4.731 ± 0.086)	(2.929 ± 0.329)
86	(1.764 ± 0.400)	(4.799 ± 0.080)	(3.034 ± 0.320)
90	(1.668 ± 0.382)	(4.854 ± 0.073)	(3.186 ± 0.309)
94	(1.549 ± 0.375)	(4.904 ± 0.069)	(3.355 ± 0.306)
98	(1.499 ± 0.365)	(4.957 ± 0.065)	(3.457 ± 0.300)
102	(1.419 ± 0.353)	(4.978 ± 0.061)	(3.559 ± 0.292)

S8 Osmotic pressure in a square lattice of DNA condensed by AuNPs

We present the osmotic pressure for the square DNA lattice condensed by 6-AuNPs or 12-AuNPs with various concentrations of monovalent salt ions ranging from c_{salt} = 0, 30, 60, 120 mM presented in Figure S9.

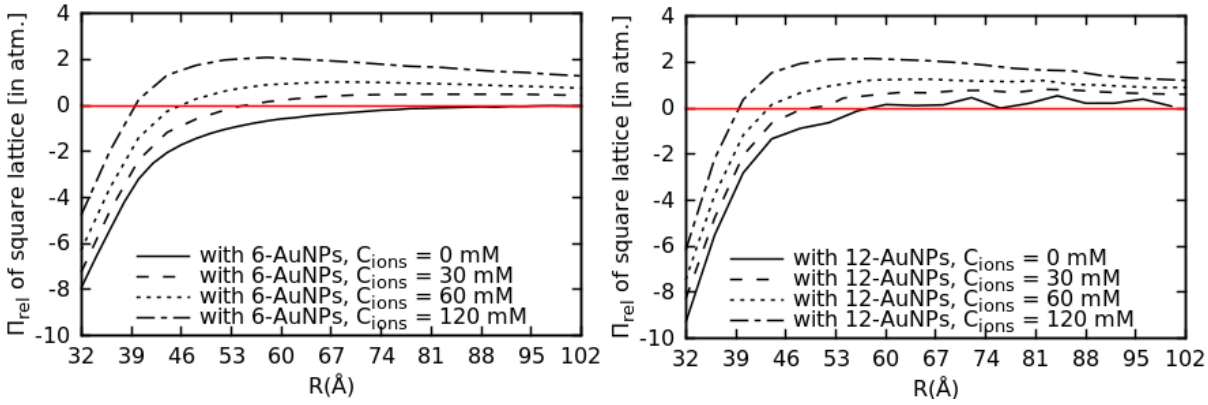

Figure S9: Relative osmotic pressure Π_{rel} (in atm or 10^5 Pa) of a square DNA lattice condensed with (left) 40 6-AuNPs or (right) 20 12-AuNPs ($R_{+/-} = 1.0$) at various salt concentrations c_s.

The profile of the osmotic pressure in the square lattice is similar to those of the hexagonal lattice presented in the main text of Section 3.3.

References

[1] M. P. Allen and D. J. Tildesley, *Computer simulation of liquids*, Oxford university press, 2017.

[2] D. Frenkel and B. Smit, *Understanding molecular simulation: from algorithms to applications*, Elsevier, 2001, vol. 1.

[3] E. Allahyarov, H. Löwen and G. Gompper, *Phys. Rev. E*, 2003, **68**, 061903.

[4] K. Besteman, K. Van Eijk and S. Lemay, *Nat. Phys.*, 2007, **3**, 641–644.

[5] E. Allahyarov, H. Löwen and G. Gompper, *Europhys. Lett.*, 2004, **68**, 894.

[6] H. Greberg and R. Kjellander, *J. Chem. Phys.*, 1998, **108**, 2940–2953.

[7] J. C. G. Montoro and J. L. Abascal, *J. Chem. Phys.*, 1998, **109**, 6200–6210.